nature portfolio

Peer Review File

Harmonization of rapid triplet up-conversion and singlet radiation enables efficient and stable white OLEDs

Reviewers' comments:

Reviewer #1 (Remarks to the Author):

The authors reported the design of high-performance all-TADF white OLEDs, in which the synergistic effect of yellow MR-TADF molecule and blue D-A type TADF molecule endows the ultrahigh power efficiency and external quantum efficiency. The photophysical and electroluminescence mechanisms are deciphered and the color tunability has also been proved. This is a piece of nice work deserving publication. I suggest the acceptance of this manuscript after carefully addressing the following issues:

Major issues:

1. The 5TCzBN could indeed trap carriers in the host matrix DMIC-TRZ. As the energy level diagram depicted, the hole trapping is dominant, and device E has shown the stronger blue emission than device C. However, the exciton recombination zone is concentrated near the electron-transporting layer at low voltage, which is conflicting to the hole-trapping feature. I think the single-carrier device of 5TCzBN: DMIC-TRZ should be examined. In addition, the effect of MR-Y on the carrier transportation should also be studied even though it had very low concentrations.

2. The discussions of the energy transfer between guest and sensitizer have some unclear issues:

(i) The kFET is highly dependent on the radiative rate of sensitizer, in which the higher kr could afford the higher kFET. As depicted in the Supplementary Table 2, the 5TCzBN possessed the nearly equal τp as the MR-Y did, from which we can preliminarily judge that the advantage of the high kr of MR-Y is actually very limited. For the direct comparison of the krs, I suggest that the authors should provide the accurate calculated data. Furthermore, I wonder if the strategy is applicable for the D-A sensitizers with lower krs?

(ii) One of the major advantages of sensitization is the elimination of exciton quenching induced by the exciton accumulation at sensitizers. In view of this point, I think the most important feature for an ideal guest material is the intrinsically high kr for preventing the exciton quenching on guest. Nevertheless, the conventional fluorescent materials also possess very high krs, even better than most MR-TADF molecules. Thus, I think the advantage of MR-TADF molecules compared to CF materials is the intrinsically higher exciton utilization, although the kRISC is not very impressive. The authors should emphasize this difference in the manuscript.

(iii) The reference of the calculation of Fŏrster energy transfer rate should be added (Fŏrster T., 10th Spiers Memorial Lecture. Transfer mechanisms of electronic excitation. Discussions of the Faraday Society, 1959, 27: 7-17.)

3. The EL performances of WOLEDs are measured with absolute EQE measurement system, which is an accurate instrument for quantum yield measurement. In that case, I wonder whether the power efficiency could be further confirmed in other instruments, such as luminance color meters and spectroradiometers.

4. The WOLEDs in the manuscript are composed of two-color components, which is not sufficient to cover the wide color gamut for realizing high color rendering index. Is this design strategy also applicable for three-color WOLEDs, in which the red MR-TADF dopant is further introduced to increase color quality?

Minor issues:

1. Fig. 2b, Fig. 3b, Fig. 5d, Supplementary figs. 5□9 are not mentioned in the manuscript.

2. The host name DMIC-TRZ is written as DMIC-Trz, in which the lower-case letter might cause the misleading and the correction is suggested for this part.

Reviewer #2 (Remarks to the Author):

The authors used the reported TADF emitters to obtain the OLEDs with broad spectrum emission by changing the doping concentration and emission region of the emission layer. The OLEDs in this work achieves a device lifetime (LT80) of 446 h at the initial luminescence of 1000 cd m-2 with a maximum external quantum efficiency of 39%, which is very impressive and attractive. However, from the CIE coordinates, the color of the devices in this work does not belong to white light, where the CIE coordinates should be located on or near at the black body radiation. Thus, the reviewer feels that this manuscript lacks rigor in data analyses. And the authors did not demonstrate any new molecular or device design strategies. Therefore, the reviewer is not able to recommend this work for publication in Nature Communications at this stage. There are some issues described blow.

1. The CIE coordinate y value of the devices in this work is approximately 0.5, which is the yellow-green range on the CIE chromaticity diagram, so these devices are not considered as white OLEDs. This is the critical issue.

2. The MR-TADF emitter MR-Y used in this work, named BNIP-tBuDPAC in the literature, is a green emitter with a PL emission peak of 544 nm and a narrow FWHM of 43 nm. Why did the authors choose this emitter? For white light emission, the emitter combination chosen by the authors clearly lacks a red component.

3. In devices A and B, the EMLs consist of 0.3 wt% and 0.5 wt% MR-Y doped into 20 wt% 5TCzBN:DMIC-TRZ, respectively. Why did the author choose these two doping concentrations? What effect does a change in doping concentration have on the photophysical properties?

4. Among these devices with complex energy transfer processes, what is the most critical factor that determines device stability? The authors should conduct a more systematic study on the relationship between device structure and stability.

5. The corresponding 5TCzBN device without MR-Y emitter should be fabricated as a reference device.

6. The authors should summarize the photophysical properties of the emission layers used in this work and present them as a table in the main text.

Reviewer #3 (Remarks to the Author):

1. In this manuscript, the authors claimed that high efficiency OLEDs with EQE of 39% and PE of 190 lm/W is achieved. However, the high efficiency can only be achieve at very low luminance. For the WOLED, the devices are always working at luminance over 2000 nit. Thus, this high efficiency is meaningless for WOLEDs. According to table S1, the EQE of the WOLEDs is only 24.1% at 1000 nit, not attractive for WOLEDs because there are several papers with better results (Nat Commun. 13, 5154 (2022); Adv.Mater. 34, 2103102 (2022); Nat Commun. 12, 3640 (2021)).

2. In line 2 on page 5, the authors claimed that the devices show high efficiency with a low efficiency roll-off. However, EQE of 39% for the OLEDs decreases down to 24.1%, and the efficiency roll off are more than 38% of the highest EQE. Why does the authors think the efficiency roll-off is low?

3. It is very significant to use color render index (CRI) to evaluate color quality of WOLEDs. But all the CRI values of WOLEDs are missing in the manuscript. Please provide the CRIs of all these WOLEDs. Furthermore, in Fig.3(e-f), the comparisons of EQEmax and PEmax versus CIEx for representative reported WOLEDs are meaningless. It would be better to compare EQEmax and PEmax versus CRI.

4. In Supplementary Fig.2, the spectral shape will change with the increase of the voltage. Why does the blue component intensity increases with the voltages? Moreover, which voltage is used to calculate the EQE value of 39%? It is well known that the spectral shape impact the efficiency.

5. The authors should provide the detail conditions to get the EL spectra (shown in the manuscript and Supplementary Fig. 4)? Also, in Table 1, please supplement the CIE/CCT test condition.

6. To demonstrate that excitons are captured directly by the guest, J-V characteristics of different concentrations are shown in Supplementary Fig. 1. However, according to the energy level diagram shown in Fig. 2(a), there is a smaller LUMO energy level offset between DMIC-TRZ and POT2T than that between 5TCzBN and POT2T, indicating the electrons are easier to inject into DMIC-TRZ from POT2T. Thus, the experimental results cannot fully support the conclusion, and more experiments should be added to interpret the carrier capture mechanism, such as the J-V characteristics of single carrier devices.

7. It is suggested to add measurements of transient EL delay curves of devices with different EMLs to provide sufficient evidence for energy transfer from 5TCzBN to MR-Y.

8. Some numerical calculation formulas and calculation processes are not clear enough, such as kr, kRISC and Forster radius R0. Please elaborate on the calculation process in the supplementary information.

9. Please supplement the current density-voltage-luminance (J-V-L) curves of all WOLEDs to better exhibit performance.

10. To investigate the spatial distribution of exciton recombination in WOLEDs, ultrathin TBRb was employed. Please provide the detail information on the ultrathin TBRB and why it is located?

Dear Editor and Reviewers,

Enclosed please find our revised manuscript entitled "**Harmonization of rapid triplet up-conversion and singlet radiation enables efficient and stable white OLEDs**" for publication as a research article in ***Nature Communications***. We sincerely thank the reviewers for their insightful and professional comments, which help us substantially improve the quality of our manuscript.

We revised the manuscript thoroughly in response to the reviewers' comments and the point-by-point responses are provided. The major improvements upon revision include:

1. A blue donor-acceptor (D-A) type TADF (*m*MDBA-DI) and orange-yellow multi-resonance (MR) TADF molecule (MR-O) are selected for improving the white color quality, leading to a standard white emission with the Commission Internationale de I'Eclairage CIE of (0.33,0.34), along with a high EQE of 35.6%.
2. The photophysical data is deeply analyzed. The calculation formulas and energy transfer process are also added in both the manuscript and supplementary information.
3. The single carrier devices are supplemented to clarify the mechanism of devices.
4. The transient electroluminescence decay test is performed and discussed in the manuscript and supplementary information.
5. The figures and tables in the manuscript and supporting information are optimized for enhanced clarity.

For your reference, annotated files of the revised manuscript and supporting information with all changes highlighted in yellow are also attached. We hope that the revised paper could now be satisfied for your requirement.

Yours Sincerely,

Chuluo Yang on behalf of the authors.

Corresponding author: **Professor Chuluo Yang**
at College of Materials Sciences and Engineering, Shenzhen University, Shenzhen 518071, People's Republic of China. Tel: +86-0755-86713985, e-mail: clyang@szu.edu.cn.

We greatly appreciate the editor and reviewers for taking the time to review and critique our manuscript. Accordingly, we have fully addressed the concerns raised by the reviewers.

Reviewer #1:

General comment: *The authors reported the design of high-performance all-TADF white OLEDs, in which the synergistic effect of yellow MR-TADF molecule and blue D-A type TADF molecule endows the ultrahigh power efficiency and external quantum efficiency. The photophysical and electroluminescence mechanisms are deciphered and the color tunability has also been proved. This is a piece of nice work deserving publication. I suggest the acceptance of this manuscript after carefully addressing the following issues:*

Response: We sincerely appreciate the reviewer's positive and professional comments.

Comment 1: *The 5TCzBN could indeed trap carriers in the host matrix DMIC-TRZ. As the energy level diagram depicted, the hole trapping is dominant, and device E has shown the stronger blue emission than device C. However, the exciton recombination zone is concentrated near the electron-transporting layer at low voltage, which is conflicting to the hole-trapping feature. I think the single-carrier device of 5TCzBN: DMIC-TRZ should be examined. In addition, the effect of MR-Y on the carrier transportation should also be studied even though it had very low concentrations.*

Response: We thank the reviewer for the constructive suggestion and apologize for the oversight. Upon clarification, it should be noted that holes are transported in the host of DMIC-TRZ rather than previously stated 5TCzBN, which can be supported by existing literature (e.g., *Nat. Commun*. **8**, 2250 (2017) and *ACS Appl. Mater. Interfaces* **9**, 4769-4777 (2017)). To substantiate our revised understanding, we tested the transient EL decay curves of related devices (Supplementary Fig. 5), which confirm the absence of spikes indicative of direct exciton trapping by 5TCzBN. This suggests that the predominant recombination mechanism is Langevin recombination occurring within the host material. Furthermore, the analysis of current density and turn-on voltages across devices with varying concentrations of 5TCzBN indicates that the 5TCzBN does not trap excitons, as these parameters remained consistent regardless of 5TCzBN concentration (Supplementary Fig. 1). Therefore, the excitons indeed form on DMIC-TRZ instead of 5TCzBN.

Following your suggestion, we constructed both a hole-only device (HOD) and an electron-only device (EOD) based on the device architectures including 0.5 wt% MR-Y:20 wt% 5TCzBN:DMIC-TRZ (Supplementary Fig. 9). The results reveal that the transport of holes exceeds that of electrons. This discrepancy in carrier transport results in the exciton recombination zone predominantly locating near the electron-transporting layer, particularly at low voltages.

Additional sentence, (manuscript, page 14): "This deduction aligns with the results from single-carrier

devices (Supplementary Fig. 9), where the hole transport is faster than the electron transport."

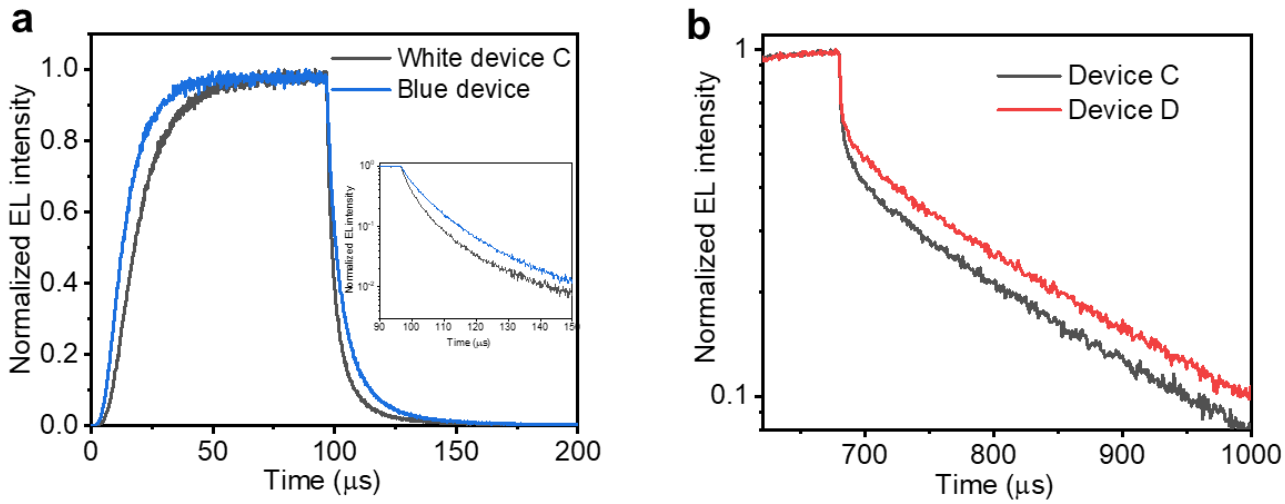

Supplementary Fig. 5. Transient EL decay curves. (a) Recorded at 490 nm with a pulse width of 200 μs for white device C and blue device based on 20 wt% 5TCzBN:DMIC-TRZ as EML (b) Recorded at 550 nm with a pulse width of 1000 μs for white device C and D. Inset: Amplified EL decay curves following the withdrawn of pulse voltages.

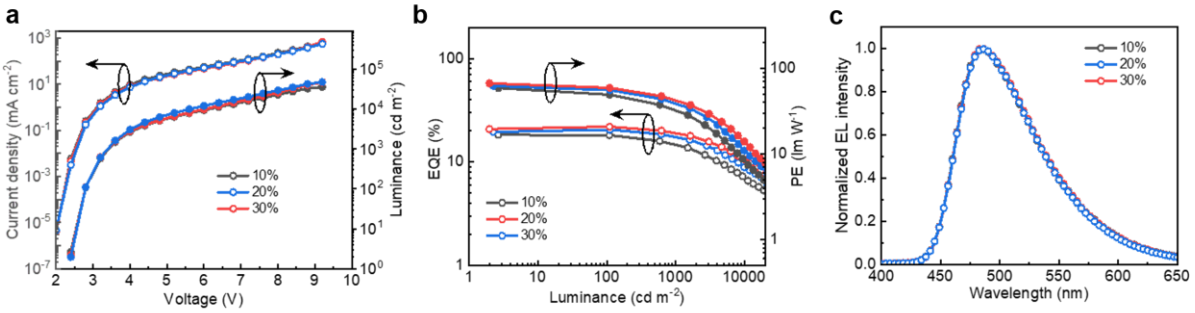

Supplementary Fig. 1. Blue OLEDs without MR-Y. (a) Current density-voltage-luminance (*J-V-L*) curves. (b) EQE and PE versus luminance characteristics. (c) Normalized electroluminescent spectra measured at 1000 cd·m^{-2} for the blue devices with different concentrations of 5TCzBN.

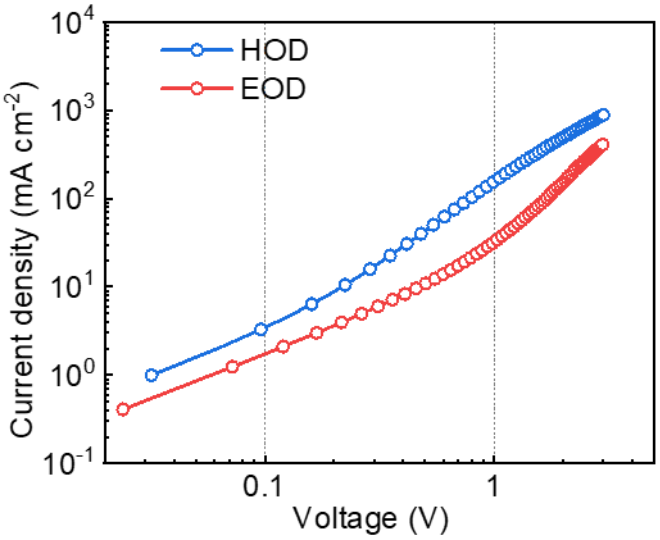

Supplementary Fig. 9. Current density-voltage characteristics of the hole-only device (HOD) and electron-only device (EOD). The device structure of the HOD and EOD were constructed as ITO/HATCN (5 nm)/TAPC (30 nm)/TCTA (15 nm)/mCBP (10 nm)/0.5 wt% MR-Y:20 wt% 5TCzBN:DMIC-TRZ (30 nm)/Al (100 nm) and ITO/0.5 wt% MR-Y:20 wt% 5TCzBN:DMIC-TRZ (30 nm)/POT2T (20 nm)/ANT-BIZ (30 nm)/Liq (2 nm)/Al (100 nm), respectively.

Comment 2: *The discussions of the energy transfer between guest and sensitizer have some unclear issues: (i) The k_{FET} is highly dependent on the radiative rate of sensitizer, in which the higher k_r could afford the higher k_{FET}. As depicted in the Supplementary Table 2, the 5TCzBN possessed the nearly equal τ_p as the MR-Y did, from which we can preliminarily judge that the advantage of the high k_r of MR-Y is actually very limited. For the direct comparison of the k_rs, I suggest that the authors should provide the accurate calculated data. Furthermore, I wonder if the strategy is applicable for the D-A sensitizers with lower k_rs?*

Response: We appreciate the reviewer for the professional suggestion. In light of the reviewer's suggestion, we re-tested all films under consistent experimental conditions, and the accurate calculated data and procedures are detailed in Table 2 and Supplementary Note 2, respectively. By analyzing the emission peaks of 5TCzBN and MR-Y at 490 nm and 550 nm respectively (Fig. 4b), we determine the $k_{r,S}$ values of 5TCzBN (1.0×10^7 s^{-1}) and MR-Y (5.4×10^7 s^{-1}). These calculations are based on the characteristic prompt lifetimes (τ_p) of 17.0 ns for 5TCzBN at 490 nm in the 20 wt% 5TCzBN:DMIC-TRZ film, and 8.1 ns for MR-Y at 550 nm in the 0.5 wt% MR-Y:DMIC-TRZ film. It is evident that the $k_{r,S}$ value of sensitizer 5TCzBN is lower than that of MR-Y, indicating the validation of employing a D-A sensitizer with a lower k_r in our study. Additionally,

we introduced a new pair of D-A type TADF sensitizer and MR-TADF emitter, namely *m*MDBA-DI and MR-O, to further validate our strategy and address the reviewer's inquiry about the applicability of D-A type TADF sensitizers with lower k_r values. The k_r of *m*MDBA-DI was found to be 0.6×10^7 s^{-1}, significantly lower than that of MR-O (7.2×10^7 s^{-1}). This demonstrates that our strategy is applicable for the D-A type TADF sensitizers with lower k_rs.

Additional section, (manuscript, Table 2):

Table 2 | Transient PL characteristic and rate constants of films.

Film	λ_{max}[a] (nm)	τ_p[b] (ns)	τ_d[b] (μs)	Φ_{PL}[c] (%)	Φ_p[d] (%)	Φ_d[d] (%)	$k_{r,S}$[e] × 10^7 (s^{-1})	k_{ISC}[e] × 10^7 (s^{-1})	k_{RISC}[e] × 10^5 (s^{-1})	k_{FET}[f] × 10^6 (s^{-1})	k_{DET}[f] × 10^5 (s^{-1})
20 wt% 5TCzBN:DMIC-TRZ	490	17.0	5.8	63	18	45	1.0	4.2	6.1	56.1	2.4
0.5 wt% MR-Y:DMIC-TRZ	550	8.1	88.0	98	44	54	5.4	6.8	0.3		
20 wt% *m*MDBA-DI:DBFPO	466	47.3	2.5	97	25	72	0.6	1.4	14.9	7.5	2.4
0.5 wt% MR-O:DBFPO	580	7.1	64.0	97	51	46	7.2	6.6	0.3		

[a] Peak wavelength of the PL spectrum in the film; [b] Lifetime of the prompt component and delayed component determined from the transient PL decay curve at 298 K; [c] Absolute photoluminescence quantum yield measured with an integration-sphere system under argon atmosphere; [d] Absolute photoluminescence quantum yield of prompt fluorescence and delayed fluorescence; [e] Rate constants of singlet radiative decay, intersystem crossing and reverse intersystem crossing. [f] Rate constants of Förster energy transfer and Dexter energy transfer.

Additional section (Supplementary Information, Supplementary Note 2):

"**Supplementary Note 2. Analyses of rate constants.**

The respective rate constants of the prompt and delayed fluorescence components (k_p and k_d) occurring in the terminal emitter, can be given by[19-22]:

$$k_p, k_d = \frac{k_{r,S} + k_{nr,S} + k_{ISC} + k_{r,T} + k_{nr,T} + k_{RISC}}{2} \times \left(1 \pm \sqrt{1 - \frac{4(k_{r,S} + k_{nr,S} + k_{ISC})(k_{r,T} + k_{nr,T} + k_{RISC}) - 4k_{ISC}k_{RISC}}{(k_{r,S} + k_{nr,S} + k_{ISC} + k_{r,T} + k_{nr,T} + k_{RISC})^2}}\right). \quad (S2)$$

k_p and k_d can be experimentally determined from prompt and delayed fluorescence decay time constants τ_p, τ_d as follows:

$$k_p = \frac{1}{\tau_p}. \quad (S3)$$

$$k_{\mathrm{d}}=\frac{1}{\tau_{\mathrm{d}}}. \quad (S4)$$

Besides, the emission quantum yields Φ_p and Φ_d for the prompt and delayed fluorescence components have the following relationship with these rate constants:

$$\Phi_{\mathrm{p}}=\frac{k_{r,S}}{k_{\mathrm{p}}}\frac{k_{r,S}+k_{nr,S}+k_{ISC}-k_d}{k_{\mathrm{p}}-k_{\mathrm{d}}}. \quad (S5)$$

$$\Phi_{\mathrm{d}}=\frac{k_{r,S}}{k_{\mathrm{d}}}\frac{k_p-k_{r,S}-k_{nr,S}-k_{ISC}}{k_{\mathrm{p}}-k_{\mathrm{d}}}. \quad (S6)$$

From the equations above, one could obtain the following relationship between rate constants and k_{p}, k_{d}, Φ_p and Φ_d experimentally determined from typical PLQY and transient PL characteristics:

$$k_{r,S}=\Phi_{\mathrm{p}}k_{\mathrm{p}}+\Phi_{\mathrm{d}}k_{\mathrm{d}}. \quad (S7)$$

$$k^S=k_{r,S}+k_{nr,S}+k_{ISC}=\frac{\Phi_{\mathrm{p}}k_{\mathrm{p}}{}^2+\Phi_{\mathrm{d}}k_{\mathrm{d}}{}^2}{k_{r,S}}. \quad (S8)$$

$$k^T=k_{r,T}+k_{nr,T}+k_{RISC}=\frac{\left(\Phi_{\mathrm{p}}+\Phi_{\mathrm{d}}\right)k_{\mathrm{p}}k_{\mathrm{d}}}{k_{r,S}}. \quad (S9)$$

$$k_{ISC}k_{RISC}=\frac{\Phi_{\mathrm{p}}\Phi_{\mathrm{d}}k_{\mathrm{p}}k_{\mathrm{d}}\left(k_{\mathrm{p}}-k_{\mathrm{d}}\right)^2}{k_{r,S}{}^2}. \quad (S10)$$

In the presence of the yellow-light-emitting component (MR-TADF emitter), the respective rate constants of the prompt and delayed fluorescence components (k_{p} and k_{d}) occurring in the blue-light-emitting component (D-A type TADF emitter), can be given by:

$$k_{\mathrm{p}},k_{\mathrm{d}}=\frac{k_{FET}+k_{r,S}+k_{nr,S}+k_{ISC}+k_{DET}+k_{r,T}+k_{nr,T}+k_{RISC}}{2}\times\left(1\pm\sqrt{1-\frac{4\left(k_{FET}+k_{r,S}+k_{nr,S}+k_{ISC}\right)\left(K_{DET}+k_{r,T}+k_{nr,T}+k_{RISC}\right)-4k_{ISC}k_{RISC}}{\left(k_{FET}+k_{r,S}+k_{nr,S}+k_{ISC}+k_{DET}+k_{r,T}+k_{nr,T}+k_{RISC}\right)^2}}\right). \quad (S11)$$

Using Vieta's formula, the sum of k_{p} and k_{d} as well as the product of k_{p} and k_{d} can be expressed as:

$$k_{\mathrm{p}}+k_{\mathrm{d}}=k_{FET}+k_{r,S}+k_{nr,S}+k_{ISC}+k_{DET}+k_{r,T}+k_{nr,T}+k_{RISC}. \quad (S12)$$

$$k_{\mathrm{p}}k_{\mathrm{d}}=\left(k_{FET}+k_{r,S}+k_{nr,S}+k_{ISC}\right)\left(k_{DET}+k_{r,T}+k_{nr,T}+k_{RISC}\right)-k_{ISC}k_{RISC}. \quad (S13)$$

By employing approximations, k_{FET} and k_{DET} can be simplified as follows:

$$k_{FET}=\frac{1}{\tau_{\mathrm{p},1}}-\frac{1}{\tau_{\mathrm{p},0}}. \quad (S14)$$

$$k_{DET}=\frac{1}{\tau_{\mathrm{d},1}}-\frac{1}{\tau_{\mathrm{d},0}}+k_{ISC}k_{RISC}\left(\tau_{\mathrm{p},1}-\tau_{\mathrm{p},0}\right). \quad (S15)$$

$\tau_{p,1}$ and $\tau_{p,0}$ represent prompt fluorescence decay times with or without guests, respectively. Likewise, $\tau_{d,1}$ and $\tau_{d,0}$ represent delayed fluorescence decay times with or without guests, respectively."

Comment 2: *(ii) One of the major advantages of sensitization is the elimination of exciton quenching induced by the exciton accumulation at sensitizers. In view of this point, I think the most important feature for an ideal guest material is the intrinsically high k_r for preventing the exciton quenching on guest. Nevertheless, the conventional fluorescent materials also possess very high k_rs, even better than most MR-TADF molecules. Thus, I think the advantage of MR-TADF molecules compared to CF materials is the intrinsically higher exciton utilization, although the k_{RISC} is not very impressive. The authors should emphasize this difference in the manuscript.*

Response: We agree with the reviewer on the importance of MR-TADF molecules' advantages over conventional fluorescent materials, particularly in terms of exciton utilization. To address this point, we have conducted a comparative study using a conventional fluorescent material, TBRb, which serves as an exemplary benchmark with its higher k_r of and emission close to that of MR-Y at 550 nm. Our results reveal that using TBRb as a yellow emitter in a device produces warm-white emission with a CIE coordinate of (0.36, 0.47). Despite the high k_r of TBRb, the external quantum efficiency (EQE) and power efficiency (PE) of this device notably decrease to 16.2% and 55 lm·W^{-1}, respectively, as shown in Fig. R1. This significant drop in device performance highlights the inefficient exciton utilization within the TBRb-based device, confirming the advantage of MR-TADF emitters.

Additional sentence, (manuscript, page 3): "Consequently, MR-TADF emitters not only offer a high k_r comparable to that of conventional fluorescent materials but also surpass them in exciton utilization efficiency, favoring higher device efficiency."

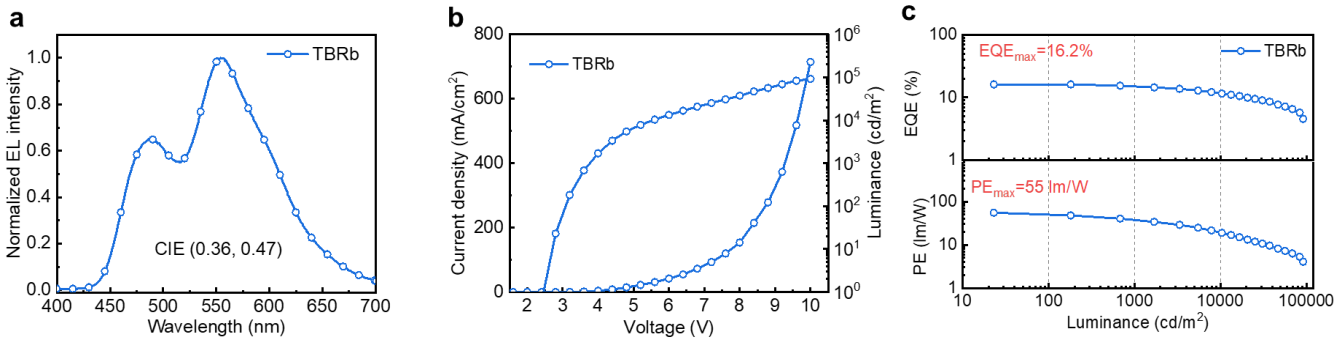

Fig. R1. WOLEDs based on TBRb as a yellow emitter. (a) Normalized electroluminescent spectra; (b)

Current density and luminance versus driving voltage characteristics; (c) EQE and PE versus luminance characteristics.

Comment 2: *(iii) The reference of the calculation of Főrster energy transfer rate should be added (Főrster T., 10th Spiers Memorial Lecture. Transfer mechanisms of electronic excitation. Discussions of the Faraday Society, 1959, 27: 7-17.)*

Response: According to your suggestion, we have added the corresponding reference in our manuscript.

Additional sentence, (manuscript, page 25): "Főrster, Th. 10th Spiers Memorial Lecture. Transfer mechanisms of electronic excitation. *Discuss. Faraday Soc.* **27**, 7-17 (1959)."

Comment 3: *The EL performances of WOLEDs are measured with absolute EQE measurement system, which is an accurate instrument for quantum yield measurement. In that case, I wonder whether the power efficiency could be further confirmed in other instruments, such as luminance color meters and spectroradiometers.*

Response: According to your suggestion, we have employed a PR735 SpectraScan Spectroradiometer along with a Keithley 2400 direct-current source meter for the measurement of the power efficiency of our devices. The supplementary data, presented in Supplementary Figs. 4 and 15, corroborates the initial results detailed in our manuscript. Specifically, the maximum power efficiency observed for devices C and G is 203 $lm \cdot W^{-1}$ and 84 $lm \cdot W^{-1}$, respectively. These values are comparable to the power efficiency values of 190 $lm \cdot W^{-1}$ and 78 $lm \cdot W^{-1}$ for the same devices as previously reported in Table 1 of our manuscript.

Modified sentence, (manuscript, page 10): "…PE of 190 $lm \cdot W^{-1}$ (confirmed at 203 $lm \cdot W^{-1}$ using a PR735 SpectraScan Spectroradiometer, Supplementary Fig. 4)"

Additional sentence, (manuscript, page 17): "Particularly, device G-1 achieves a maximum EQE of 35.8% and a maximum PE of 78 $lm \cdot W^{-1}$ (confirmed at 84 $lm \cdot W^{-1}$ using a PR735 SpectraScan Spectroradiometer, Supplementary Fig. 15) at a voltage of 3.6 V (Fig. 6c), with the corresponding CIE coordinate of (0.33, 0.34) locating at blackbody radiation curve."

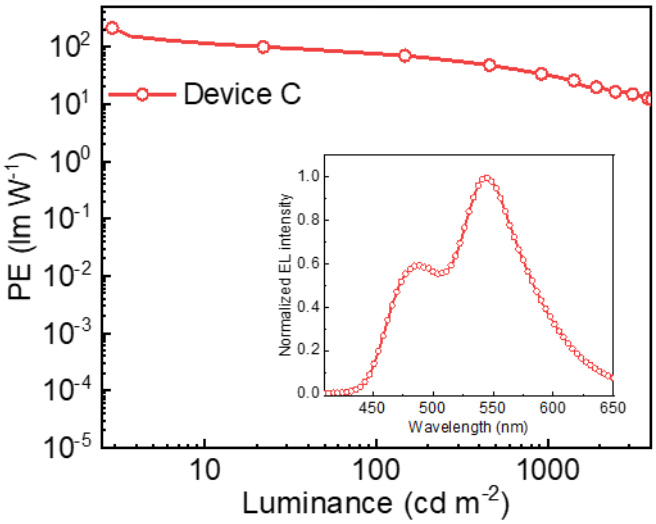

Supplementary Fig. 4. PE versus luminance characteristics of devices C. Tested by a PR735 SpectraScan Spectroradiometer and a Keithley 2400 direct-current source meter. Inset: Normalized electroluminescent spectra at 1000 cd·m^{-2}.

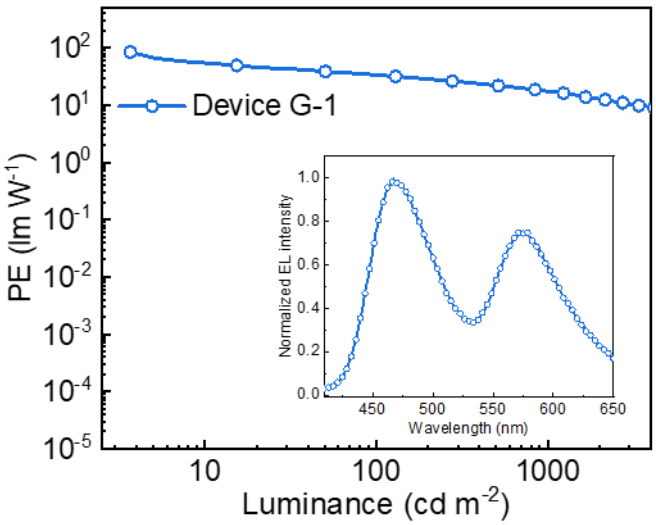

Supplementary Fig. 15. PE versus luminance characteristics of device G-1. Tested by a PR735 SpectraScan Spectroradiometer and a Keithley 2400 direct-current source meter. Inset: Normalized electroluminescent spectra at 1000 cd·m^{-2}.

Comment 4: *The WOLEDs in the manuscript are composed of two-color components, which is not sufficient to cover the wide color gamut for realizing high color rendering index. Is this design strategy also applicable for three-color WOLEDs, in which the red MR-TADF dopant is further introduced to increase color quality?*

Response: We appreciate the reviewer's insightful comment. In the updated version of our manuscript, we demonstrate that a WOLED constructed from two color components is sufficient to cover a wide color gamut and achieve a high color rendering index. This is accomplished through the integration of a new blue D-A type TADF emitter and a new orange-yellow MR-TADF emitter, as detailed in Fig. 6.

In exploring the applicability of our design strategy for three-color WOLEDs, we tested the incorporation of a red MR-TADF dopant into our device configuration. As illustrated in Fig. R2, we introduced a 5 nm thick red emissive layer (EML) between the existing EML and the hole-blocking layer (HBL). This red EML contains 20 wt% MCPPSeZ and 0.5 wt% BNO1, doped into the DMIC-TRZ host. The MCPPSeZ, an efficient D-A type TADF emitter with its rapid k_{RISC} of 4.2×10^6 s^{-1} (*Chem. Eng. J.* **482**, 149150 (2024)), and BNO1, a highly efficient red MR-TADF emitter with a high $k_{r,S}$ of 7.4×10^7 s^{-1} (*Adv. Mater.* **34**, 2201442 (2022)), serve as the sensitizer and emitter, respectively, aligning with our design strategy. This three-color WOLED achieves commendable efficiencies, with a maximum EQE of 30.6% and a PE of 107 $lm \cdot W^{-1}$. However, the device exhibits a less optimal CIE coordinate of (0.51, 0.43), mainly due to exciton trapping within the red EML. Given the complexity introduced by adding a third color component, it may be worthwhile to conduct a separate study to thoroughly investigate the applicability of our design strategy in three-color WOLEDs.

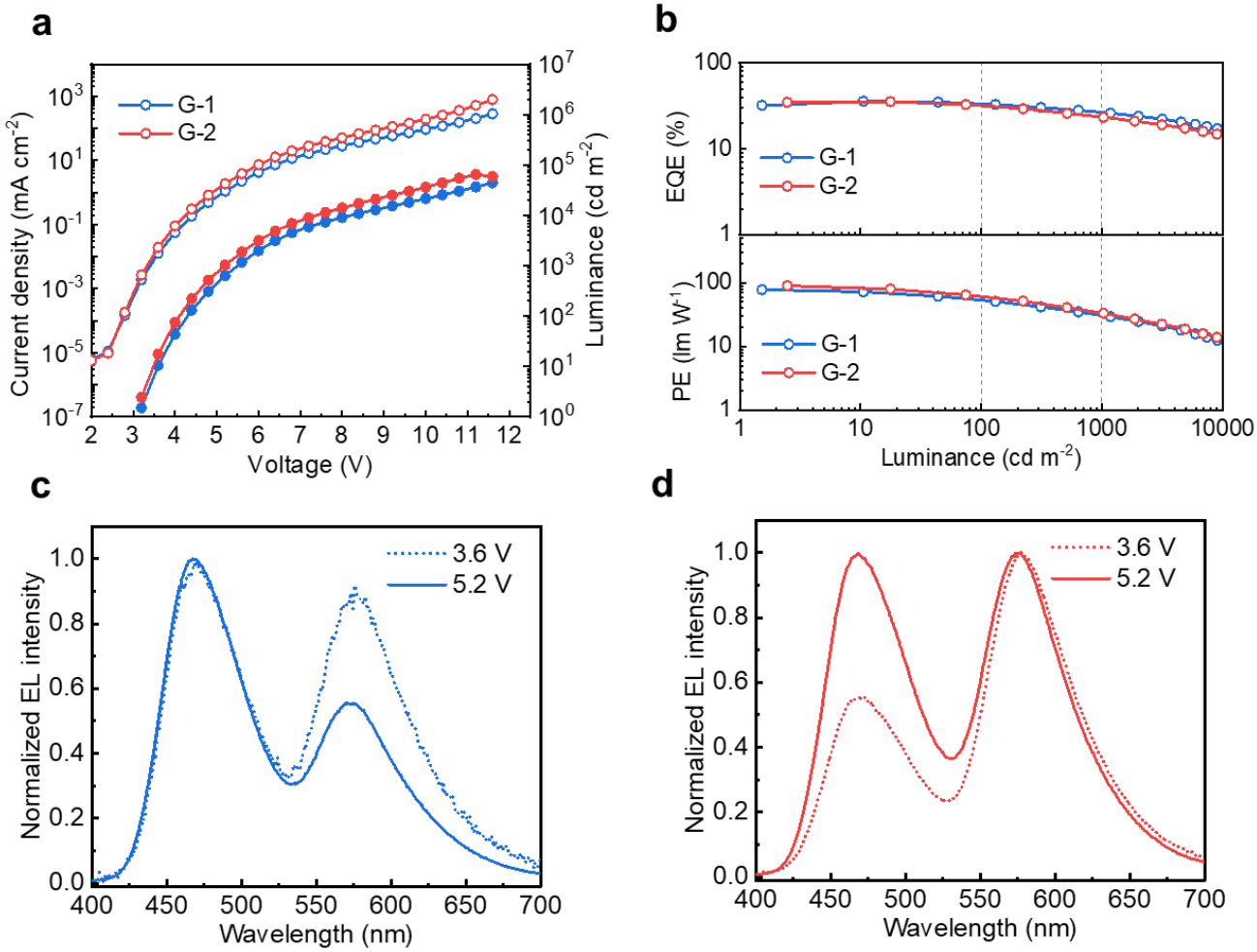

Fig. 6 | Standard white OLED (devices G1~2). a, Current density and luminance versus voltage characteristics. **b**, EQE and PE versus luminance characteristics. **c**,**d**, Normalized electroluminescent spectra measured at 3.6 V and 5.2 V for device G-1 (**c**) and device G-2 (**d**) (Note: The devices exhibit peak efficiency at 3.6 V and reach a brightness of 1000 cd·m^{-2} at 5.2 V).

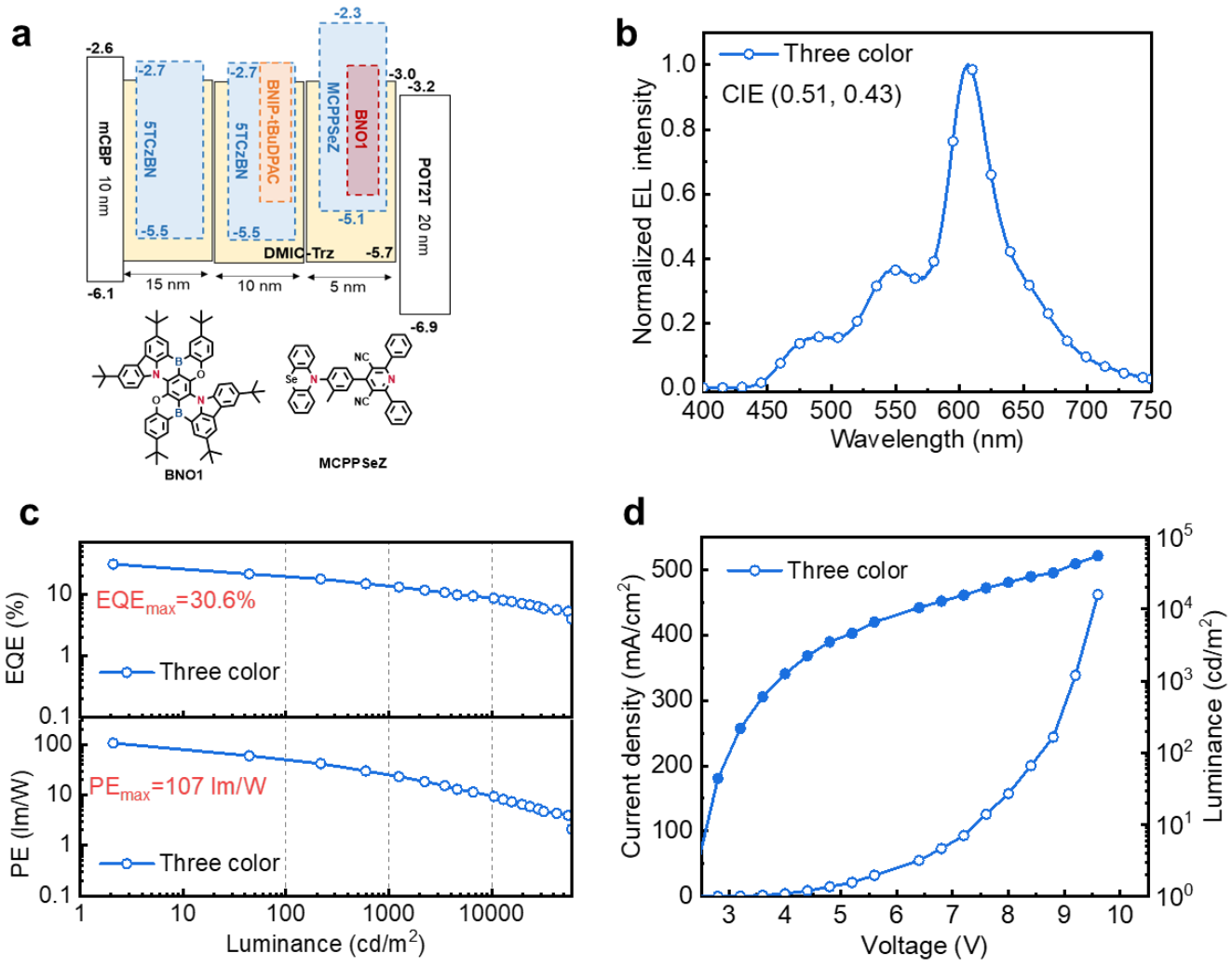

Fig. R2. Three-color WOLEDs. a, Device architectures. **b**, Normalized electroluminescent spectra. **c**, EQE and PE versus luminance characteristics. **d**, Current density-voltage-luminance curves.

Minor issues:

1. Fig. 2b, Fig. 3b, Fig. 5d, Supplementary figs. 5–9 are not mentioned in the manuscript.

Response: Thanks for the reminder. Correlative figures and expressions have been one-to-one correspondence, as follows:

(Manuscript, page 7) "the chemical structures of the relevant materials are shown in Fig. 2b"

(Manuscript, page 10) "maintaining a remarkable PE of 190 $lm \cdot W^{-1}$ (confirmed at 203 $lm \cdot W^{-1}$ using a PR735 SpectraScan Spectroradiometer, Supplementary Fig. 4) and an unprecedented EQE of 39% (Figs. 3b and 3c)"

(Manuscript, page 16) "showing a transition from warm white emission to warmer white emission (Fig. 5d)."

Supplementary Fig. 5, originally depicting the cyclic voltammetry curve of 5TCzBN, is removed due to

redundancy. Supplementary Figs. 6 and 7 from the original version have been merged to form the new Supplementary Fig. 6, providing a clearer presentation. Supplementary Figs. 8 and 9 in the original version have been renumbered due to the addition of a new Supplementary Figure and now correspond to Supplementary Figs. 7 and 11, respectively. All Supplementary Figures are mentioned in the manuscript.

(Manuscript, page 12) "we fabricated four thin films: pristine DMIC-TRZ, 0.5 wt% MR-Y:DMIC-TRZ, 20 wt% 5TCzBN:DMIC-TRZ, and 0.5 wt% MR-Y:20 wt% 5TCzBN:DMIC-TRZ for collecting the transient PL decay curves (Figs. 4b-4d and Supplementary Fig. 6)"

(Manuscript, page 14) "Due to the fine overlap between the absorption spectrum of TBRb and the PL spectrum of 5TCzBN (Supplementary Fig. 7)"

(Manuscript, page 16) "As anticipated, all four devices achieve similar PEs of approximately 190 $lm \cdot W^{-1}$ (Supplementary Fig. 11 and Table 1)"

2. The host name DMIC-TRZ is written as DMIC-Trz, in which the lower-case letter might cause the misleading and the correction is suggested for this part.

Response: According to the reviewer's suggestion, we unify host name as DMIC-TRZ and modify it in Fig. 5a and Fig. 5c.

Reviewer #2:

General comment: *The authors used the reported TADF emitters to obtain the OLEDs with broad spectrum emission by changing the doping concentration and emission region of the emission layer. The OLEDs in this work achieve a device lifetime (LT_{80}) of 446 h at the initial luminescence of 1000 cd m^{-2} with a maximum external quantum efficiency of 39%, which is very impressive and attractive. However, from the CIE coordinates, the color of the devices in this work does not belong to white light, where the CIE coordinates should be located on or near at the black body radiation. Thus, the reviewer feels that this manuscript lacks rigor in data analyses. And the authors did not demonstrate any new molecular or device design strategies. Therefore, the reviewer is not able to recommend this work for publication in Nature Communications at this stage. There are some issues described below.*

Response: Thank you for your critical comment and constructive suggestion. While there is no new molecular design, our work introduces a distinct and previously unexplored combination of existing materials, aimed at surpassing current limitations in WOLED performance. Traditionally, MR-TADF emitters, due to their narrow emission linewidth, are considered less suitable for WOLED applications, which necessitate a broad emission spectrum ranging from 400 to 700 nm. Our research advances this field by integrating MR-TADF emitters with high k_r as the yellow-light component, paired uniquely with D-A type TADF molecules characterized by rapid k_{RISC} as the blue-light component. This combination aiming at WOLEDs provides pivotal scientific insights along with exceptional device efficiency.

In the updated version of our manuscript, we have corrected our description of previous WOLEDs to 'warm-white OLEDs', aligning with the terminology of existing literature within the *Nature* family and other highly reputable journals (e.g., *Nat. Photon.* **18**, 200–206 (2024); *Nat. Commun.* **13**, 6495 (2022); *Nat. Commun.* **13**, 5154 (2022); *Nat. Commun.* **12**, 1421 (2021); *Adv. Mater.* **32**, 2004040 (2020)). In addition, to be more rigorous, we successfully constructed a device emitting 'pure' white light with standard white light coordinates (0.33, 0.34) and exceptional performance (EQE_{max} = 35.6%), based on our well-considered design approach. Furthermore, we have enriched our manuscript with additional data on thin films and comparative devices, providing comprehensive scientific insights. This includes in-depth analyses of thin-film photophysical data and device data with varying concentrations of yellow MR-TADF dopant as well as device performance solely utilizing the D-A type TADF emitter. We explore, in detail, the relationship between device structure and stability, underscoring the significance and ingenuity of our design. We hope to have thoroughly addressed the reviewer's concerns and demonstrated the manuscript's suitability for publication in *Nature*

Communications.

Comment 1: *The CIE coordinate y value of the devices in this work is approximately 0.5, which is the yellow-green range on the CIE chromaticity diagram, so these devices are not considered as white OLEDs. This is the critical issue.*

Response: We sincerely appreciate the reviewer's constructive comment. In the updated version of our manuscript, we have successfully developed white OLEDs (Fig. 6) that not only showcase exceptional performance (EQE_{max} = 35.6%) but also achieve the desired CIE coordinate of (0.33, 0.34), precisely on the blackbody radiation curve. This is accomplished through the integration of a blue D-A type TADF molecule (*m*MDBA-DI), emitting at 466 nm with faster k_{RISC} of 14.9 × 10^5 s^{-1}, and an orange-yellow MR-TADF molecule (MR-O), emitting at 580 nm with higher $k_{r,S}$ of 7.2 × 10^7 s^{-1}, further substantiating the viability of our proposed approach for the construction of WOLEDs.

Moreover, we have updated our manuscript to more accurately describe our previous WOLEDs as "warm-white OLEDs", aligning with terminologies recognized in the existing literature. For instance, Zhao et al. have described dual-color devices W1-6 with CIE coordinates of (0.374, 0.505) as warm-white OLEDs (*Nat. Commun.* **13**, 5154 (2022)). Similarly, Wang et al. referred to their devices with CIE coordinates of (0.44, 0.53) as warm-white LEDs (*Nat. Commun.* **12**, 1421 (2021)). Furthermore, several experimental studies have categorized white light observations with the CIE coordinate y value near 0.5 as warm-white light emission (*Nat. Commun.* **13**, 6495 (2022); *Adv. Mater.* **32**, 2004040 (2020)). These findings have been cited to justify our initial use of the term "warm-white" in the manuscript. Indeed, a CIE coordinate y value close to 0.5 corresponds to the yellow-green range on the CIE chromaticity diagram, evidenced by photographs of warm-white LEDs (Fig. R3 in *Nat. Photon.* **18**, 200-206 (2024)). However, our warm-white OLEDs appear more akin to white light to the human eye due to the closer alignment of the CIE coordinate x value to 0.33, as shown in the inset of Fig. 3d. This observation led to our initial description of the devices as white OLEDs, supported by literature wherein devices described as emitting white light actually fall within the warm-white region (*Nature* **459**, 234-238 (2009); *Adv. Mater.* **35**, 2208361 (2023)). We believe our updated manuscript conducts a more precise analysis and discussion of the data, addressing the critical issue as highlighted by the reviewer.

Additional paragraph, (manuscript, page 16):

"In pursuit of standard white emission targeting a CIE of (0.33, 0.33) and high color rendering index (CRI),

we introduced the bluer D-A type TADF emitter of 5-(3,11-dimethyl-5,9-dioxa-13*b*-boranaphtho[3,2,1-*de*]anthracen-7-yl)-10,15-diphenyl-10,15-dihydro-5*H*-diindolo[3,2-*a*:3′,2′-*c*]carbazole[41] (*m*MDBA-DI), which features a faster k_{RISC} of 14.9 × 10^5 s^{-1} (Supplementary Fig. 13, Supplementary Fig. 14 and Table 2), for the fabrication of devices G-1 and G-2. The device structure is ITO/HAT-CN (5 nm)/TAPC (30 nm)/TCTA (15 nm)/mCBP (10 nm)/EML (30 nm)/DBFPO (10 nm)/ANT-BIZ (30 nm)/Liq (2 nm)/Al (100 nm). In devices G-1 and G-2, the EML consists of 0.3 wt% and 0.5 wt% MR-O doped into 20 wt% *m*MDBA-DI:DBFPO, where DBFPO (Dibenzo[*b*,*d*]furan-2,8-diylbis(diphenylphosphine oxide)), with a higher triplet energy (T_1 = 3.1 eV) than DMIC-TRZ (T_1 = 2.8 eV), serves as a suitable host for the bluer emitter *m*MDBA-DI (T_1 = 2.9 eV). As shown in Fig. 6 and Table 1, both devices exhibit a high maximum EQE of over 35%, indicating efficient exciton utilization in the devices. However, the maximum PE of 90 $lm \cdot W^{-1}$ is deemed unsatisfactory due to the elevated turn-on voltages (from 2.2 V to 3.0 V) necessitated by the high triplet energy host (DBFPO). Particularly, device G-1 achieves a maximum EQE of 35.8% and a maximum PE of 78 $lm \cdot W^{-1}$ (confirmed at 84 $lm \cdot W^{-1}$ using a PR735 SpectraScan Spectroradiometer, Supplementary Fig. 15) at a voltage of 3.6 V (Fig. 6c), with the corresponding CIE coordinates of (0.33, 0.34) locating at blackbody radiation curve. Conversely, device G-2, under a drive voltage of 5.2 V (Fig. 6d), manages to approach standard white light emission with CIE coordinates of (0.33, 0.34) and an EQE of 25.9% at 1,000 $cd \cdot m^{-2}$, which is apparently the most efficient WOLEDs with a CIE of x and y values both close to 0.33 at the practical brightness level reported so far[8,13,31] (Supplementary Fig. 16 and Supplementary Table 4). This demonstrates that standard white light emission can be attained through careful optimization of material selection, doping concentration, and voltage adjustments. Furthermore, both devices G-1 and G-2 achieve a CRI of approximately 70, indicating excellent color quality for two-color WOLEDs. These outcomes highlight the effectiveness of our approach by employing MR-TADF emitters with high k_r as yellow-light components and D-A type TADF molecules with rapid k_{RISC} as blue-light

components, offering a robust platform for advancing WOLED technology."

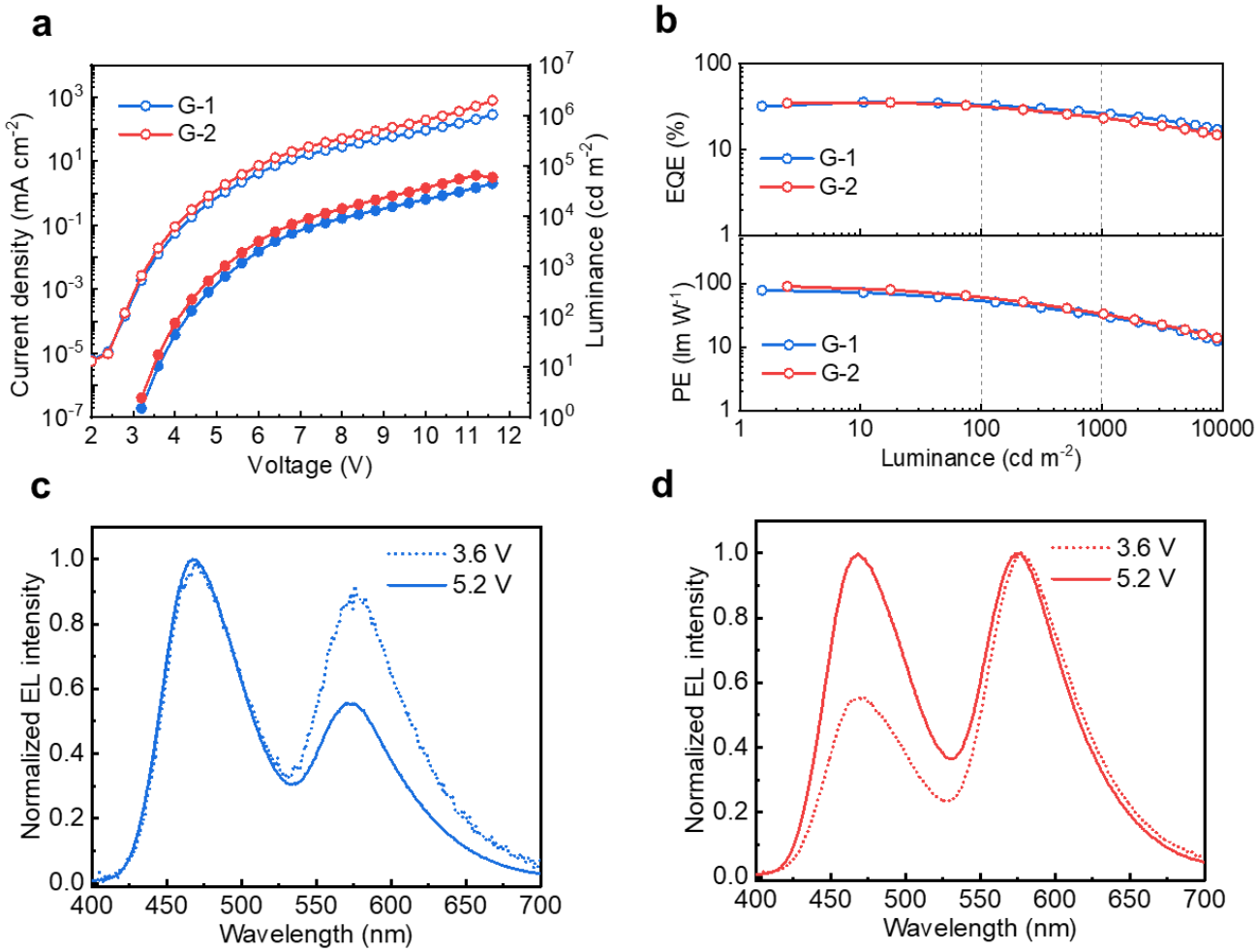

Fig. 6 | Standard white OLED (devices G1~2). **a**, Current density and luminance versus voltage characteristics. **b**, EQE and PE versus luminance characteristics. **c**,**d**, Normalized electroluminescent spectra measured at 3.6 V and 5.2 V for device G-1 (**c**) and device G-2 (**d**) (Note: The devices exhibit peak efficiency at 3.6 V and reach a brightness of 1000 cd·m^{-2} at 5.2 V).

Fig. R3. A photograph of warm-white LEDs in *Nat. Photon.* **18**, 200-206 (2024)

Comment 2: *The MR-TADF emitter MR-Y used in this work, named BNIP-tBuDPAC in the literature, is a green emitter with a PL emission peak of 544 nm and a narrow FWHM of 43 nm. Why did the authors choose this emitter? For white light emission, the emitter combination chosen by the authors clearly lacks a red component.*

Response: We appreciate the reviewer for the professional comment. As noted in a highly cited TADF review (*Adv. Mater.* **29**, 1605444 (2017)), green-to-yellow emitters are defined by their electroluminescence peak wavelength ranging between 500 nm and 580 nm. Thus, a wavelength of 540 nm is widely accepted as the dividing line between green and yellow emitters, a delineation supported by the existing literature (*Adv. Mater.* **29**, 1605444 (2017); *Angew. Chem. Int. Ed.* ***55***, 7998 (2016); *Angew. Chem. Int. Ed.* **59**, 7063 (2020)). BNIP-tBuDPAC exhibits a photoluminescence emission peak at 544 nm with a narrow full-width at half-maximum (FWHM) of 43 nm when dissolved in toluene at a concentration of 10^{-5} mol·L^{-1}. However, when incorporated into the device, the electroluminescence peak shifts to 554 nm and the FWHM broadens to 58 nm, characteristics aligning with its classification as a yellow emitter. The selection of BNIP-tBuDPAC is driven by its notable characteristics: a highly efficient yellow emission, characterized by high k_r of 5.4×10^7 s^{-1}, and remarkable quantum yield of 98%. These properties fit our design approach perfectly, as we require a yellow emitter capable of rapidly converting energy received from the blue emitter into yellow light, a process essential for achieving the desired color balance in our device.

To address the reviewer's concern regarding the lack of a red component, we explored the fabrication of a three-color WOLED (for details, see our response to **Comment 4** from **Reviewer 1**). The incorporation of a red component, while still maintaining commendable device performance, results in a deviation from the expected CIE coordinates mainly due to exciton trapping in the red EML.

To achieve the desired white light emission in the device, we introduced another orange-yellow MR-TADF molecule with a higher k_r (7.2×10^7 s^{-1}) than BNIP-tBuDPAC and peak emission wavelength at 580 nm. Paired with a blue D-A type TADF molecule featuring faster k_{RISC} (14.9×10^5 s^{-1}) and an emission peak at 466 nm, the resulting device realizes white light emission with standard white light coordinates (0.33, 0.34) as per our proposed approach.

Comment 3: *In devices A and B, the EMLs consist of 0.3 wt% and 0.5 wt% MR-Y doped into 20 wt%*

5TCzBN:DMIC-TRZ, respectively. Why did the author choose these two doping concentrations? What effect does a change in doping concentration have on the photophysical properties?

Response: We appreciate the reviewer for the professional comment. Achieving white light emission in our bi-chromatic devices necessitates a delicate balance between the k_r of the blue component and the k_{FET} from the blue to the yellow component. Specifically, the selection of low doping concentrations for the yellow component optimizes the intermolecular distance (R) between blue and yellow components, ensuring k_{FET} does not exceed k_r. This is of particular importance as k_{FET} is highly sensitive to R, evidenced by the relationship: $k_{FET} = k_r \frac{J\kappa^2}{R^6}(\frac{9000(ln10)}{128\pi^5 N_A n^4})$. The particular doping concentrations of 0.3 wt% and 0.5 wt% for the yellow component are chosen based on their impact on their electroluminescence spectra at a brightness of 1000 cd·m^{-2} (Supplementary Fig. 3a). At 0.5 wt% doping level, the device exhibits predominant yellow light emission. Reducing MR-Y concentration to 0.3 wt% results in a more balanced blue and yellow light emission. However, this balance comes at the cost in reduced device efficiency. Further reduction of the doping concentration to 0.2% does not result in significant chromatic enhancement and brings additional challenges in the device fabrication process. Thus, in our initial submission, we chose 0.3 wt% and 0.5 wt% doping concentrations to prepare devices A and B, which allowed us to evaluate our proposed approach effectively.

In response to the concerns raised, and to ensure the clarity and integrity of our presentation, we have investigated the photophysical properties of films with 0.3 wt% and 0.5 wt% MR-Y doping within 20 wt% 5TCzBN:DMIC-TRZ matrix (Supplementary Figs. 3b and 3c). A rise in doping concentration is observed to result in a significant decrease in the blue light emission and a shorter emission lifetime at 490 nm. This confirms that a higher doping concentration of the yellow component indeed promotes FET from the blue to the yellow component, consistent with our experimental findings for the devices.

Additional sentence, (manuscript, page 7): "Furthermore, diminishing the doping ratio to 0.2% does not yield substantial chromatic enhancements, while concurrently bringing challenges in the device preparation process (Supplementary Fig. 3)."

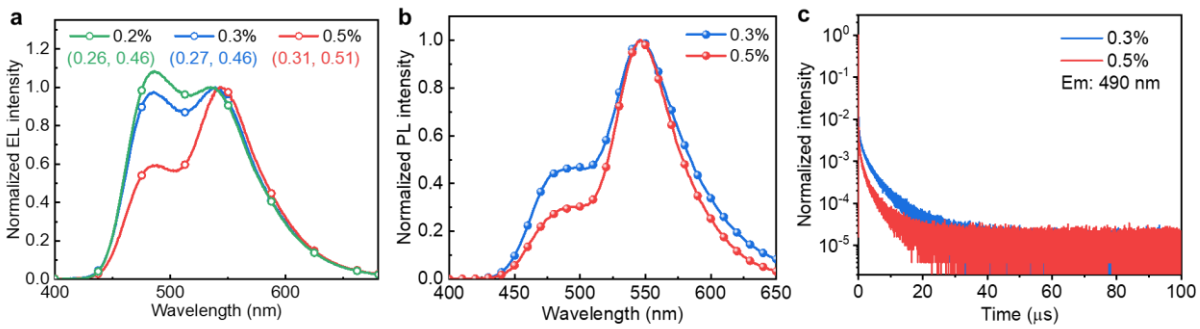

Supplementary Fig. 3. Comparison for devices and films with different doping ratios of MR-Y. (a) Normalized electroluminescent spectra at 1000 $cd \cdot m^{-2}$ for devices with 0.2, 0.3 and 0.5 wt% doping concentrations of MR-Y. (b) PL spectra and (c) Transient PL decay curves of films with 0.3 wt% and 0.5 wt% MR-Y doping in the 20 wt% 5TCzBN:DMIC-TRZ matrix at the emission wavelength of 490 nm.

Comment 4: *Among these devices with complex energy transfer processes, what is the most critical factor that determines device stability? The authors should conduct a more systematic study on the relationship between device structure and stability.*

Response: We thank the reviewer for raising the professional comment. Device stability is affected by several interrelated factors, such as material purity, chemical bond strength, interface interactions, and the accumulation of triplet excitons. It is imperative to understand that these factors are interconnected and difficult to distinguish the most critical one. In our initial submission, we opted to maintain relative structural uniformity across the devices while variably adjusting the doping of 5TCzBN in devices C and D to manipulate the energy transfer pathway. Obviously, device C with 5TCzBN to decrease the accumulation of triplet excitons exhibits a nearly 4.5 times longer lifetime than that of device D without 5TCzBN. This deliberate strategy enables us to explore the impact of triplet excitons on device stability with a focused approach.

Comment 5: *The corresponding 5TCzBN device without MR-Y emitter should be fabricated as a reference device.*

Response: According to the reviewer's suggestion, we have fabricated a reference device containing 5TCzBN without the MR-Y emitter (Supplementary Fig. 1 and Supplementary Table 1) and added the description prior to the preparation of our WOLEDs.

Additional paragraph, (manuscript, page 6):

"Prior to fabricating WOLED devices, we investigated the performance of blue devices without doping MR-Y, using the following structure: indium-tin oxide (ITO)/1,4,5,8,9,11-hexaazatriphenylenehexacarbonitrile (HAT-CN, 5 nm)/1,1-bis[(di-4-tolylamino)phenyl]cyclohexane (TAPC, 30 nm)/tris(4-carbazolyl-9-ylphenyl)amine (TCTA, 15 nm)/3,3-di(9*H*-carbazol-9-yl)biphenyl (mCBP, 10 nm)/emitting layer (EML, 30 nm)/(1,3,5-triazine-2,4,6triyl)tris(benzene-3,1-diyl)(tris(diphenylphosphine oxide)) (POT2T, 20 nm)/1-(4-(10-([1,1'-biphenyl]-4-yl)anthracen-9-yl)phenyl)-2-ethyl-1H-benzo[*d*]imidazole (ANT-BIZ, 30 nm)/8-hydroxyquinolinato lithium (Liq, 2 nm)/alumina (Al, 100 nm). In this configuration, HAT-CN serves as the hole injection layer, while both TAPC and TCTA act as the hole transporting layers. ANT-BIZ functions as the electron transporting layer. To confine exciton diffusion, mCBP and POT2T are employed as the electron-blocking layer and hole-blocking layer, respectively. The emitting layer consists of blue emitter of 5TCzBN and host of 1,3-dihydro-1,1dimethyl-3-(3-(4,6-diphenyl-1,3,5-triazin-2-yl)phenyl)indeno[2,1-*b*]carbazole (DMIC-TRZ). These blue devices exhibit an emission peak at 490 nm with EQEs ranging from 18.3% to 22.0%. Notably, the device featuring a 20 wt% doping of 5TCzBN demonstrates the highest efficiency and minimal efficiency roll-off, as depicted in Supplementary Fig. 1 and Supplementary Table 1."

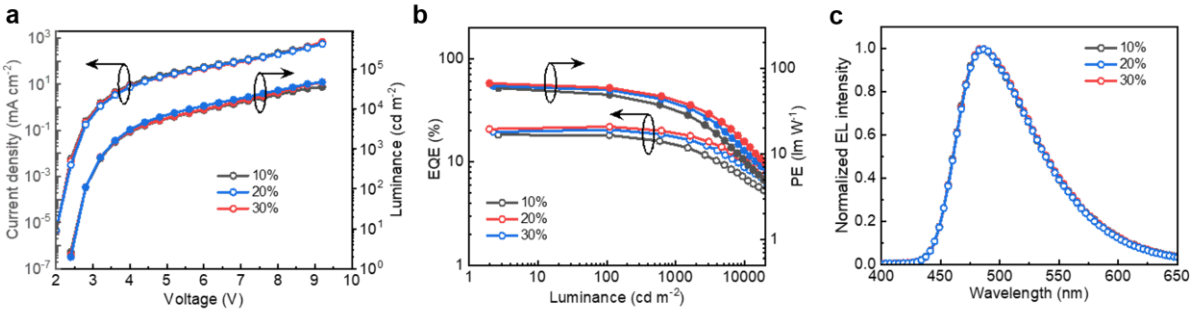

Supplementary Fig. 1. Blue OLEDs without MR-Y. (a) Current density-voltage-luminance (*J-V-L*) curves. (b) EQE and PE versus luminance characteristics. (c) Normalized electroluminescent spectra measured at 1000 cd·m^{-2} for the blue devices with different concentrations of 5TCzBN.

Supplementary Table 1. Key data for blue OLEDs.

Ratio	V_{on} (V)[a]	EQE (%)[b]	PE (lm·W^{-1})[c]	L_{max} (cd·m^{-2})[d]	EL (nm)[e]
10%	2.2	18.3	59	36020	490
20%	2.2	22.0	67	47676	490
30%	2.2	20.6	63	47186	490

[a] Turn-on voltage at 1.0 cd·m^{-2}; [b] Maximum external quantum efficiency; [c] Maximum power efficiency; [d] Maximum luminance; [e] Electroluminescence peak wavelength at 1,000 cd m^{-2}.

Comment 6: *The authors should summarize the photophysical properties of the emission layers used in this work and present them as a table in the main text.*

Response: We appreciate the reviewer for the professional suggestion. Following this advice, we have detailed the photophysical properties of the emission layers utilized in our work within **Table 2** of the updated manuscript.

Additional table, (manuscript, **Table 2**):

Table 2 | Transient PL characteristic and rate constants of films.

Film	λ_{max}[a] (nm)	τ_p[b] (ns)	τ_d[b] (μs)	Φ_{PL}[c] (%)	Φ_p[d] (%)	Φ_d[d] (%)	$k_{r,S}$[e] × 10^7 (s^{-1})	k_{ISC}[e] × 10^7 (s^{-1})	k_{RISC}[e] × 10^5 (s^{-1})	k_{FET}[f] × 10^6 (s^{-1})	k_{DET}[f] × 10^5 (s^{-1})
20 wt% 5TCzBN:DMIC-TRZ	490	17.0	5.8	63	18	45	1.0	4.2	6.1	56.1	2.4
0.5 wt% MR-Y:DMIC-TRZ	550	8.1	88.0	98	44	54	5.4	6.8	0.3		
20 wt% *m*MDBA-DI:DBFPO	466	47.3	2.5	97	25	72	0.6	1.4	14.9	7.5	2.4
0.5 wt% MR-O:DBFPO	580	7.1	64.0	97	51	46	7.2	6.6	0.3		

[a] Peak wavelength of the PL spectrum in the film; [b] Lifetime of the prompt component and delayed component determined from the transient PL decay curve at 298 K; [c] Absolute photoluminescence quantum yield measured with an integration-sphere system under argon atmosphere; [d] Absolute photoluminescence quantum yield of prompt fluorescence and delayed fluorescence; [e] Rate constants of singlet radiative decay, intersystem crossing and reverse intersystem crossing. [f] Rate constants of Förster energy transfer and Dexter energy transfer.

Reviewer #3:

Comment 1: *In this manuscript, the authors claimed that high efficiency OLEDs with EQE of 39% and PE of 190 lm/W is achieved. However, the high efficiency can only be achieved at very low luminance. For the WOLED, the devices are always working at luminance over 2000 nit. Thus, this high efficiency is meaningless for WOLEDs. According to table S1, the EQE of the WOLEDs is only 24.1% at 1000 nit, not attractive for WOLEDs because there are several papers with better results (Nat Commun. 13, 5154 (2022); Adv. Mater. 34, 2103102 (2022); Nat Commun. 12, 3640 (2021)).*

Response: We appreciate the reviewer for the constructive suggestions. In revising our manuscript, we have meticulously addressed the concerns raised, particularly focusing on the performance of our WOLEDs at practical brightness level (1000 nit). In the updated version of our manuscript, we report that our devices achieve 'pure' white light emission with standard white light coordinates (0.33, 0.34), demonstrating an impressive maximum external quantum efficiency (EQE) of 35.6% and maintaining an EQE of 25.9% at 1000 nit. Our analysis, as detailed in Supplementary Fig. 16 and Supplementary Table 4, demonstrates that while our EQE at 1000 nit may not be the highest value, the combined consideration of EQE and CIE coordinates (*x* and *y* values) at this brightness level positions our devices advantageously compared to those from several papers mentioned by the reviewer. Additionally, power efficiency (PE) is another crucial metric for the evaluation of WOLEDs, particularly at practical brightness level (1000 nit). In our initial submission, our WOLEDs achieved a PE of 82 $lm \cdot W^{-1}$ at this brightness level. This performance is comparable to the highest PE of 83.5 $lm \cdot W^{-1}$ at 1000 nit, as mentioned in several papers referenced by the reviewer (Supplementary Table 4). Further, when considered alongside their close-to-ideal CIE coordinates (*x* and *y* values close to 0.33) at this brightness, our WOLEDs not only match but in some cases exceed the performance reported in the referenced studies (Supplementary Fig. 16). Moreover, our research endeavors to advance beyond the current state of the art by employing an approach previously unexplored that harmonizes rapid k_{RISC} of D-A type TADF molecules and high k_r of MR-TADF molecules. This approach addresses the previously considered challenge of MR-TADF emitters due to their narrow emission spectrum, traditionally considered unsuitable for WOLEDs that require broad spectral coverage from 400 to 700 nm. Our intention in this work is to propose a simple, universally applicable approach for achieving WOLEDs, providing significant scientific insights together with exceptional device efficiency. This not only represents an important advance in OLED research but also greatly enhances the commercial prospects of WOLED technology.

Additional sentences (manuscript, page 17): "Conversely, device G-2, under a drive voltage of 5.2 V (Fig.

6d), manages to approach standard white light emission with CIE coordinates of (0.33, 0.34) and an EQE of 25.9% at 1,000 cd·m^{-2}, which is apparently the most efficient WOLEDs with a CIE of x and y values both close to 0.33 at the practical brightness level reported so far[8,13,31] (Supplementary Fig. 16 and Supplementary Table 4).”

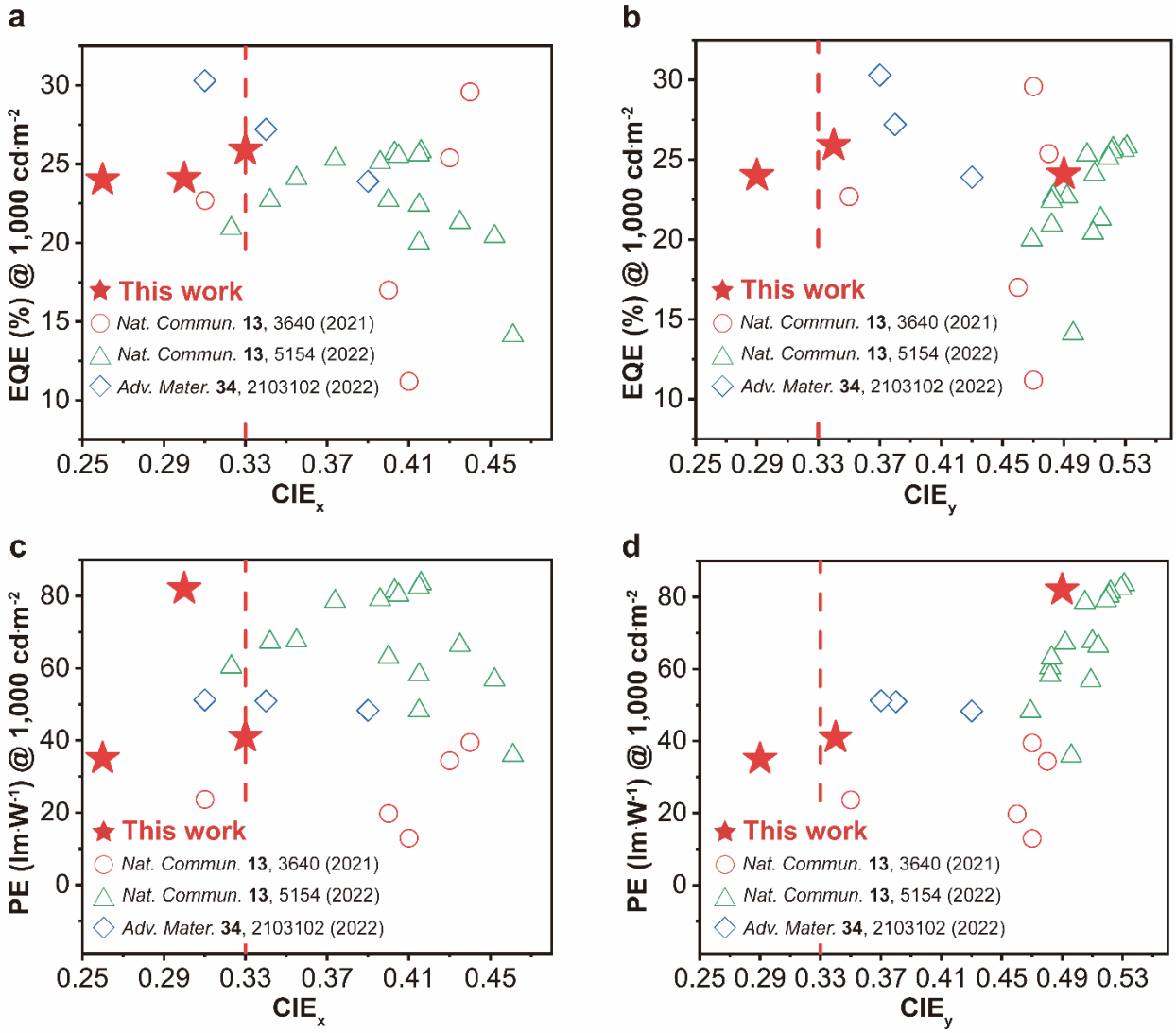

Supplementary Fig. 16. Comparison of EQE, PE, and CIE with representative reports. (a) EQE$_{1000}$ versus CIE$_x$ coordinates at the luminance of 1,000 cd·m^{-2}. (b) EQE$_{1000}$ versus CIE$_y$ coordinates at the luminance of 1,000 cd·m^{-2}. (c) PE$_{1000}$ versus CIE$_x$ coordinates at the luminance of 1,000 cd·m^{-2}. (d) PE$_{1000}$ versus CIE$_y$ coordinates at the luminance of 1,000 cd·m^{-2}.

Supplementary Table 4. Comparison of the key performance data of representative reports and this work.

Ref.	EQE[a] (%)	PE[b] ($lm \cdot W^{-1}$)	CIE[c] (x, y)	Device structure
This work	39.0/24.1	190/82	(0.30,0.49)	HATCN|TAPC|TCTA|mCBP|DMIC-TRZ:20% 5TCzBN|DMIC-TRZ:20% 5TCzBN:0.5% MR-Y|POT2T|ANT-BIZ|Liq
	35.8/24.0	78/35	(0.26,0.29)	HATCN|TAPC|TCTA|mCBP|DBFPO:20% *m*MDBA-DI| DBFPO:20% *m*MDBA-DI:0.3% MR-O|DBFPO|ANT-BIZ|Liq
	35.6/25.9	90/41	(0.33,0.34)	HATCN|TAPC|TCTA|mCBP|DBFPO:20% *m*MDBA-DI| DBFPO:20% *m*MDBA-DI:0.5% MR-O|DBFPO|ANT-BIZ|Liq
Nat. Commun. **12**, 3640 (2021)	30.6/25.4	98.4/34.4	(0.43,0.48)	MoO_3|mCP|mCP:*p*DPBITPO:35% DMAC-DPS:0.5% 4CzTPNBu|*p*DPBITPO|LiF
	26.5/22.7	74.4/23.7	(0.31,0.35)	MoO_3|mCP|mCP:*Dp*PBITPO:35% DMAC-DPS:0.2% 4CzTPNBu|*pD*PBITPO|LiF
	32.7/29.6	108.2/39.5	(0.44,0.47)	MoO_3|mCP|mCP:*Dp*PBITPO:35% DMAC-DPS:0.5% 4CzTPNBu|*pD*PBITPO|LiF
	25.0/11.2	82.7/13.0	(0.41,0.47)	MoO_3|mCP|mCP:*pD*PBITPO:35% DMACDPS:0.5% 4CzTPNBu|*pD*PBITPO|LiF (10 in^2)
	26.1/17.0	86.6/19.8	(0.40,0.46)	MoO_3|mCP|mCP:*Dp*PBITPO:35% DMACDPS:0.5% 4CzTPNBu|*pD*PBITPO|LiF (10 in^2)
Nat. Commun. **13**, 5154 (2022)	27.7/24.1	111.0/67.6	(0.355,0.510)	HATCN|TAPC|TcTa|mCP|TCP-BP-SFAC| TCP-BP-SFAC:1% 4CzTPNBu|PPF|TmPyPB|LiF
	28.8/25.8	117.0/83.5	(0.416,0.531)	HATCN|TAPC|TcTa|mCP|TCP-BP-SFAC| TCP-BP-SFAC:1% 4CzTPNBu|TCPBP-SFAC|PPF|TmPyPB|LiF
	29.1/25.6	120.4/82.4	(0.415,0.529)	HATCN|TAPC|TcTa|mCP|TCP-BP-SFAC| TCP-BP-SFAC:1% 4CzTPNBu|TCPBP-SFAC|PPF|TmPyPB|LiF
	30.0/25.7	122.5/81.4	(0.403,0.522)	HATCN|TAPC|TcTa|mCP|TCP-BP-SFAC|TCP-BP-SFAC:1% 4CzTPNBu|TCPBP-SFAC|PPF|TmPyPB|LiF
	30.0/25.5	121.2/80.3	(0.405,0.521)	HATCN|TAPC|TcTa|mCP|TCP-BP-SFAC|TCP-BP-SFAC:1 % 4CzTPNBu|TCPBP-SFAC|PPF|TmPyPB|LiF
	30.2/25.1	122.6/79.0	(0.396,0.519)	HATCN|TAPC|TcTa|mCP|TCP-BP-SFAC| TCP-BP-SFAC:1 4CzTPNBu|TCPBP-SFAC|PPF|TmPyPB|LiF
	31.1/25.3	130.7/78.5	(0.374,0.505)	HATCN|TAPC|TcTa|mCP|TCP-BP-SFAC|TCP-BP-SFAC:1% 4CzTPNBu|TCPBP-SFAC|PPF|TmPyPB|LiF
	30.2/22.7	127.4/67.2	(0.342,0.492)	HATCN|TAPC|TcTa|mCP|TCP-BP-SFAC| TCP-BP-SFAC:1% 4CzTPNBu|TCPBP-SFAC|PPF|TmPyPB|LiF
	27.5/20.9	110.4/60.4	(0.323,0.482)	HATCN|TAPC|TcTa|mCP|TCP-BP-SFAC| TCP-BP-SFAC:1% 4CzTPNBu|TCPBP-SFAC|PPF|TmPyPB|LiF
	30.9/22.7	110.7/63.1	(0.400,0.483)	HATCN|TAPC|TcTa|Mcp| TCP-BP-SFAC:1% DBP|TCP-BPSFAC:1.5% 4CzTPNBu|TCP-BP-SFAC|PPF|TmPyPB|LiF
	29.1/22.4	99.7/58.2	(0.415,0.482)	HATCN|TAPC|TcTa|mCP|TCP-BP-SFAC:1% DBP|TCP-BPSFAC:1.5% 4CzTPNBu|TCP-BP-SFAC|PPF|TmPyPB|LiF
	29.6/20.0	92.4/48.2	(0.415,0.469)	HATCN|TAPC|TcTa|mCP|TCP-BP-SFAC:1% DBP/TCP-BPSFAC:1.5% 4CzTPNBu|TCP-

				BP-SFAC|PPF|TmPyPB|LiF
	26.0/21.3	101.7/66.4	(0.435,0.514)	MoO_3|mCBP|DIC-TRZ:1.5% 4CzTPNBu|TCP-BP-SFAC:20% BCz-TRZ|TPBi|Bpy-TP2|LiF
	24.3/20.4	97.5/56.8	(0.452,0.509)	MoO_3|mCBP|DIC-TRZ:1% DBP| DIC-TRZ:1.5% 4CzTPNBu|TCP-BPSFAC:20% BCz-TRZ|TPBi|Bpy-TP2|LiF
	22.8/14.1	82.4/35.9	(0.461,0.496)	MoO_3|mCBP|DIC-TRZ:1% DBP|DIC-TRZ:1.5% 4CzTPNBu|TCP-BPSFAC:20% BCz-TRZ|TPBi|Bpy-TP2|LiF
Adv. Mater. **34**, 2103102 (2022)	24.3/23.9	53.7/48.3	(0.39,0.43)	HATCN|NPB|TCTA|32aICTRZ:15% DACz-TAZTRZ|mCPBC:10% TDBA-DI|CzPhPy|p-bPPhen|LiF
	28.0/27.2	58.3/50.9	(0.34,0.38)	HATCN|NPB|TCTA|32aICTRZ:15% DACz-TAZTRZ|mCPBC:10% TDBA-DI|CzPhPy|p-bPPhen|LiF
	30.7/30.3	57.7/51.2	(0.31,0.37)	HATCN|NPB|TCTA|32aICTRZ:15% DACz-TAZTRZ|mCPBC:10% TDBA-DI|CzPhPy|p-bPPhen|LiF

[a]External quantum efficiency: maximum, values at 1,000 $cd \cdot m^{-2}$; [b]Power efficiency: maximum, values at 1,000 $cd \cdot m^{-2}$; [c]Commission Internationale de l'Eclairage coordinates at 1,000 $cd \cdot m^{-2}$.

Comment 2: *In line 2 on page 5, the authors claimed that the devices show high efficiency with a low efficiency roll-off. However, EQE of 39% for the OLEDs decreases down to 24.1%, and the efficiency roll off are more than 38% of the highest EQE. Why does the authors think the efficiency roll-off is low?*

Response: We appreciate the reviewer for the professional suggestion and regret any confusion caused, due to unclear comparisons in our initial submission. The statement about low efficiency roll-off specifically refers to the comparison between device C, which includes a D-A type TADF molecule as a sensitizer in the Y-EML, and device D, which lacks this sensitizer.

Modified sentences (manuscript, page 5): "…accompanied by an improved efficiency roll-off compared to the device without D-A type TADF molecule as sensitizer."

Comment 3: *It is very significant to use color render index (CRI) to evaluate color quality of WOLEDs. But all the CRI values of WOLEDs are missing in the manuscript. Please provide the CRIs of all these WOLEDs. Furthermore, in Fig.3(e-f), the comparisons of EQE_{max} and PE_{max} versus CIE_x for representative reported WOLEDs are meaningless. It would be better to compare EQE_{max} and PE_{max} versus CRI.*

Response: We thank the reviewer for the valuable suggestion. In our initial submission, we emphasized the significance of both x and y values of the CIE coordinates for WOLEDs, a point specifically highlighted by **Reviewer 2**. We presented comparisons of EQE_{max} and PE_{max} versus the CIE_x of WOLEDs to inform readers of our efforts in simultaneously enhancing the EQE and PE of WOLEDs while also improving their CIE_x values. To address the concerns raised, we have provided the CRI values for all the WOLEDs we prepared, as presented in Table 1. We have also included comparisons of EQE_{max} and PE_{max} versus CRI, as presented in Supplementary Table 2 and Fig. R4.

In the updated manuscript version, we have successfully developed WOLEDs (designated as devices G-1 and G-2) that not only meet the standard white light coordinates (0.33, 0.34) but also exhibit high EQE_{max} up to 35.6%, PE_{max} up to 90 $lm \cdot W^{-1}$, and a commendable CRI of about 70. Additionally, by analyzing the experimental results of previously reported WOLEDs in Supplementary Table 2, we observe that achieving a high CRI in WOLEDs often necessitates compromises in other performance metrics, such as EQE and PE, sometimes even affecting the CIE coordinates. This observation is corroborated by the experimental results from our devices. A comparison (Fig. R4) of EQE_{max} and PE_{max} versus CRI demonstrates that our WOLED devices G-1 and G-2 exhibit the highest EQE and PE among WOLEDs with CRIs approaching or exceeding 70.

Table 1 | Summary of the key performance data of WOLEDs.

Device	V_{on} (V)[a]	EQE (%)[b]	PE (lm·W^{-1})[c]	L_{max} (cd.m^{-2})[d]	CIE[e]	CCT (K)[e]	CRI[e]
A	2.2	32.7/24.0	158/74	84009	(0.27, 0.46)	7217	41
B	2.2	35.9/27.6	184/95	127385	(0.31, 0.51)	5954	40
C	2.2	39.0/24.1	190/82	98134	(0.30, 0.49)	6343	41
D	2.2	38.5/16.3	196/52	103379	(0.33, 0.51)	5569	42
C-1	2.2	37.4/19.6	183/65	76662	(0.28, 0.47)	6833	42
C-2	2.2	38.5/22.7	194/79	105801	(0.30, 0.49)	6310	42
C-3	2.2	38.8/27.6	195/100	146016	(0.33, 0.52)	5616	40
C-4	2.2	37.1/30.7	194/112	129386	(0.35, 0.53)	5218	38
E	2.6	29.3/22.9	101/58	104673	(0.26, 0.46)	7444	42
F-1	2.4	34.5/18.9	117/44	111200	(0.38, 0.45)	4353	54
F-2	2.4	35.0/20.4	117/48	109769	(0.44, 0.46)	3362	47
F-3	2.2	33.6/16.7	130/41	67392	(0.30, 0.42)	6385	56
F-4	2.2	37.2/18.8	144/49	87713	(0.37, 0.45)	4632	56
G-1	3.0	35.8/26.0	78/35	64647	(0.26, 0.29)	120000	71
G-2	3.0	35.6/25.9	90/41	64647	(0.33, 0.34)	5583	69

[a] Turn-on voltage at 1 cd·m^{-2}; [b] External quantum efficiency: maximum, values at 1,000 cd·m^{-2}; [c] Power efficiency: maximum, values at 1,000 cd·m^{-2}; [d] Maximum luminance; [e] Commission Internationale de l'Eclairage coordinates, correlated color temperature and color rendering index at 1,000 cd·m^{-2}.

Supplementary Table 2. Summary performances for representative WOLEDs.

Type	Ref.	V_{on} [a](V)	EQE[b] (%)	PE[c] (lm·W^{-1})	CIE[d]	CRI[e]	LT[f] @1,000 cd·m^{-2}
All Fluo.	This work	2.2	39.0/24.1	190/82	(0.40,0.57)/(0.30,0.49)	41	446 (LT_{80})
		3.0	35.8/26.0	78/35	(0.33,0.34)/(0.26,0.29)	71	
		3.0	35.6/25.9	90/41	(0.41,0.39)/(0.33,0.34)	69	
	Nat. Commun. **10**, 2380 (2019)[1]	2.6	20.5%/13%	59.6/31.7	NA/(0.33,0.41)	72	380† (LT_{80})
	Nat Commun. **12**, 3640 (2021)[2]	2.7	32.7%/29.6%	108.2/39.5	NA/(0.44,0.47)	NA	50† (LT_{80})
	Adv. Funct. Mater. **30**, 2005165 (2020)[3]	2.7	21.9%/19.8%	76.7/36.1	NA/(0.39,0.48)	69	
	Adv. Funct. Mater. 2209163 (2022)[4]	2.6	27.2%/23.6%	108.6/42.7	NA/(0.37,0.48)	NA	
	Adv. Mater. **28**, 3122-3130 (2016)[5]	3.9	19.1/15.7	40.6/-	NA/(0.32,0.43)	NA	
	Adv. Mater. **32**, 1906950 (2020)[6]	3.1	23.6%/20.7%	55.1/18.1	NA/(0.34,0.36)	87	
	Chem. Eng.J. **392**, 124870 (2020)[7]	2.8	20.4%/16.9%	62.8/25.3	NA/(0.35,0.45)	72	
	Chem. Sci. **12**, 14519 (2021)[8]	2.9	24.2%/20.9%	70.8/30	NA/(0.28,0.39)	NA	0.2 (LT_{50})
	Adv.Mater. **34**, 2103102 (2022)[9]	-	30.7%/30.3%	57.7/51.2	(0.40,0.47)/(0.31,0.37)	76	402 (LT_{80})
	Nat Commun. **13**, 5154 (2022)[10]	2.5	31.1%/25.3%	130.7/78.5	NA/(0.37,0.51)	NA	
	ACS Appl. Mater. Interfaces **13**, 44615 (2021)[11]	3.2	23.5%/-	55.5/-	NA/(0.29,0.36)	71	
	Adv. Funct. Mater. **31**, 2101647 (2021)[12]	2.6	32.8%/24.1%	99.9/-	NA/(0.41,0.46)	60	

All Phos.	*Adv. Funct. Mater.* **27**, 1701314 (2017)[13]	2.5	28.1/21.5	105/59.5	NA/(0.40,0.48)	NA	
	J. Appl. Phys. **115**, 244512 (2014)[14]	2.7	22.3/22.0	64.8/55.1	NA/(0.42,0.45)	60	
Hybrid Fluo. & Phos.	*Adv. Funct. Mater.* **31**, 2100704 (2021)[15]	2.6	25.4/25.2	71/49.7	NA/(0.51,0.42)	84	
	J. Mater. Chem. C **8**, 6577 (2020)[16]	2.6	23.6/18.3	68.8/38.1	NA/(0.49,0.43)	NA	600 (LT_{50})
	Adv. Mater. **35**, 2208361 (2023)[17]	/	24.5/24.3	64.0/49.2	NA/(0.54,0.41)	50	17,687 (LT_{95})
	J. Mater. Chem. C **8**, 7543 (2020)[18]	2.6	23.6/20.0	77.8/49.5	NA/(0.47,0.41)	37	

[a] Turn-on voltage at 1cd·m^{-2}; [b] External quantum efficiency: maximum, values at 1,000 cd·m^{-2}; [c] Power efficiency: maximum, values at 1,000 cd·m^{-2}; [d] Commission Internationale de l'Eclairage coordinates at maximum EQE and 1,000 cd·m^{-2}, respectively; [e] Color rendring index at 1,000 cd·m^{-2}; [f] Operational time at an initial luminance of 1,000 cd·m^{-2}; † These numbers were estimated from the data or figures in the reference papers.

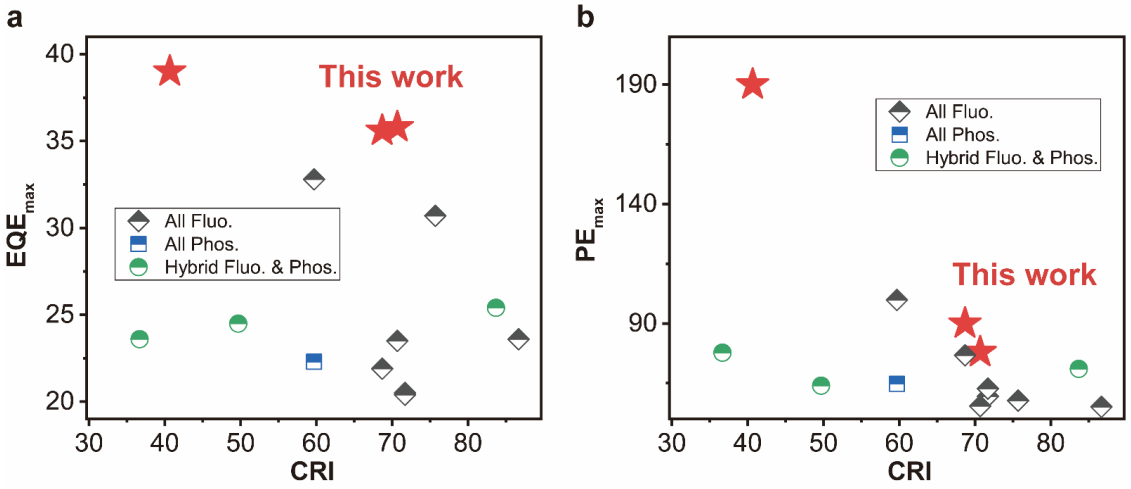

Fig. R4. Comparison of EQE and PE with representative reports. (a) EQE versus CRI. (b) PE versus CRI.

Comment 4: *In Supplementary Fig.2, the spectral shape will change with the increase of the voltage. Why does the blue component intensity increase with the voltages? Moreover, which voltage is used to calculate the EQE value of 39%? It is well known that the spectral shape impacts the efficiency.*

Response: We appreciate the reviewer for the insightful comment. As the voltage increases, both the exciton recombination zone broadens and the exciton density rises, leading to an enhanced intensity of the blue light component. This increase in intensity is similarly observed in the yellow light component, as now detailed in Supplementary Fig. 8 of the revised supplementary information. The EQE value of 39% is achieved under the specific voltage of 2.4 V.

We also wish to highlight a key advancement in our study: the substitution of the emitters in our WOLEDs. Specifically, we replaced the blue D-A type TADF emitter (5TCzBN) and yellow MR-TADF emitter (MR-Y) in device C with bluer D-A type TADF emitter (*m*MDBA-DI) and orange-yellow MR-TADF emitter (MR-O) in device G-1 and G-2, respectively. This strategic change is to achieve high efficiency at a specific voltage where the spectral shape is close to white emission. Notably, device G-1 achieved a maximum EQE value of 35.8% at 3.6 V, with corresponding CIE coordinates of (0.33, 0.34) at this low voltage (Fig. 6).

Additional sentences (Manuscript, page 14): "Our findings indicate that at lower operating voltages, the exciton recombination zone predominantly localizes near the electron-transporting layer. As the voltage increases, this recombination zone distributes more uniformly across the entire EML."

Modified sentences (Manuscript, page 14): "…consequently enhancing the emission intensity of both the blue and yellow light components (Supplementary Fig. 8)."

Additional sentences (Manuscript, page 17): "Particularly, device G-1 achieves a maximum EQE of 35.8%

and a maximum PE of 78 $lm \cdot W^{-1}$ (confirmed at 84 $lm \cdot W^{-1}$ using a PR735 SpectraScan Spectroradiometer, Supplementary Fig. 15) at a voltage of 3.6 V (Fig. 6c), with the corresponding CIE coordinates of (0.33, 0.34) locating at blackbody radiation curve."

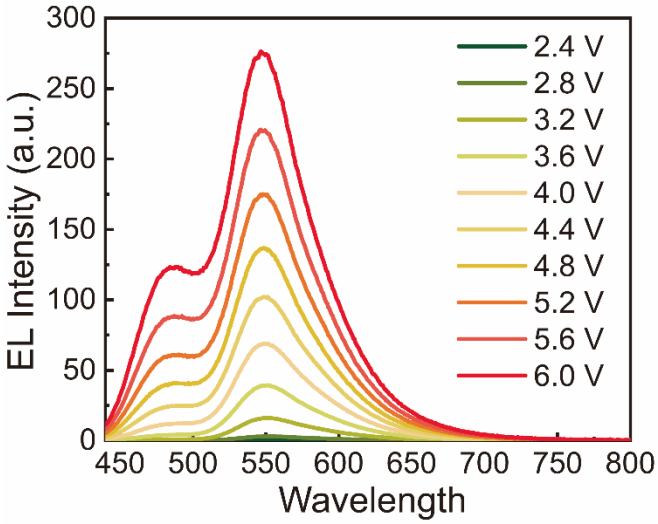

Supplementary Fig. 8. Electroluminescent spectra of device C under the operational voltages ranging from 2.4 to 6.0 V.

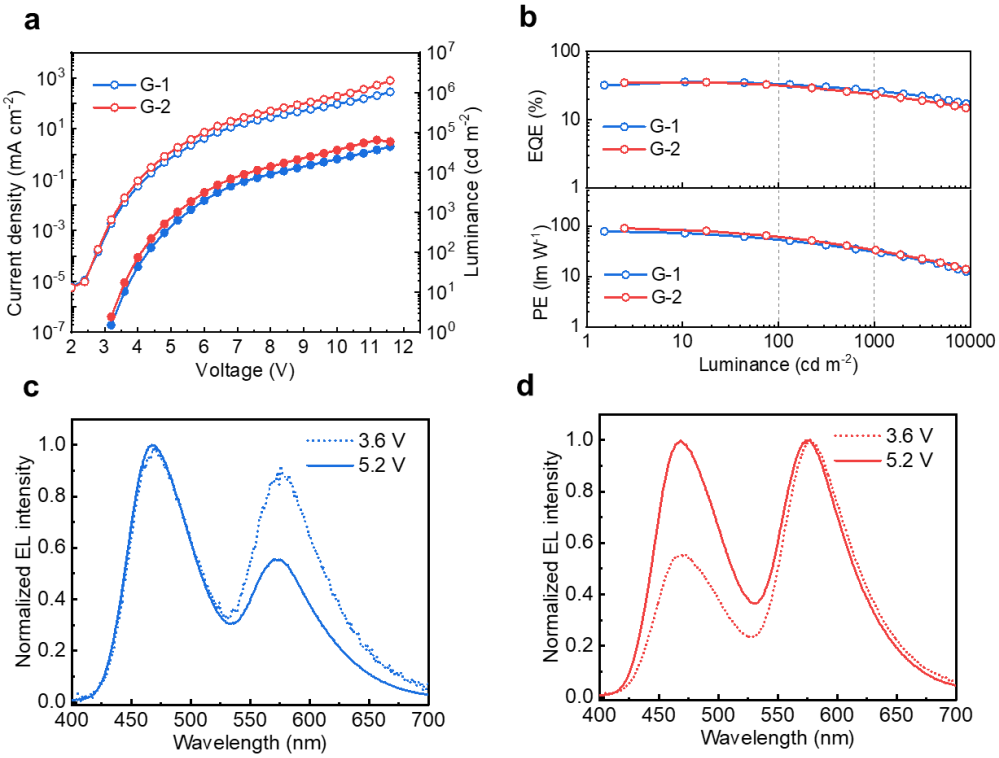

Fig. 6 | Standard white OLED (devices G1~2). a, Current density and luminance versus voltage characteristics. **b**, EQE and PE versus luminance characteristics. **c**,**d**, Normalized electroluminescent spectra measured at 3.6 V and 5.2 V for device G-1 (**c**) and device G-2 (**d**) (Note: The devices exhibit peak efficiency at 3.6 V and reach a brightness of 1000 $cd \cdot m^{-2}$ at 5.2 V).

Comment 5: *The authors should provide the detail conditions to get the EL spectra (shown in the manuscript and Supplementary Fig. 4)? Also, in Table 1, please supplement the CIE/CCT test condition.*

Response: We appreciate the reviewer for these constructive suggestions. Accordingly, we have clarified the measurement conditions for the EL spectra in the legends of Figs. 2, 3, 5 and all supplementary figures. We have also supplemented the measurement conditions for the CIE/CCT in the note of Table 1. These measurements are conducted at a luminance of 1000 $cd \cdot m^{-2}$.

Additional legend (manuscript, Fig. 2 and Fig. 3): "Normalized electroluminescent spectra tested at 1000 $cd \cdot m^{-2}$."

Additional legend (manuscript, Fig. 5): "Normalized electroluminescent spectra of devices C-1~4 measured at 1000 $cd \cdot m^{-2}$."

Additional note (manuscript, Table 1): "Commission Internationale de I'Eclairage coordinates, correlated color temperature and color rendering index at 1,000 $cd \cdot m^{-2}$."

Comment 6: *To demonstrate that excitons are captured directly by the guest, J-V characteristics of different concentrations are shown in Supplementary Fig. 1. However, according to the energy level diagram shown in Fig. 2(a), there is a smaller LUMO energy level offset between DMIC-TRZ and POT2T than that between 5TCzBN and POT2T, indicating the electrons are easier to inject into DMIC-TRZ from POT2T. Thus, the experimental results cannot fully support the conclusion, and more experiments should be added to interpret the carrier capture mechanism, such as the J-V characteristics of single carrier devices.*

Response: We are thankful to the reviewer for the professional observation and appreciate the opportunity to thoroughly review our experimental data. Upon re-evaluation, it is important to clarify that excitons predominantly form on the host material DMIC-TRZ rather than on 5TCzBN as previously mentioned. It appears that current density-voltage curves of the blue device containing 10 wt% 5TCzBN in the previous submission was abnormal, likely an artifact of our device fabrication or measurement setup. In response, we conduct a statistical analysis on datasets to confirm the consistency and reliability of our results. We notice that the "10% 1st" dataset presented initially is an outlier due to its significant deviation from the other two datasets ("10% 2nd" and "10% 3rd") under the same device structure (Fig. R5). Based on statistical grounds, we have thus excluded this anomalous data from our analysis. Further detailed evaluations of the effective datasets reveal that the current density-voltage curves, both at high voltage (displayed on a linear scale in the Fig. R5a) and at low voltage (displayed on an exponential scale in the Fig. R5b), remain consistent regardless

of the concentration of 5TCzBN. Besides, the turn-on voltage is consistently at 2.2 V across varying concentrations, further confirming that 5TCzBN does not act as a trap for excitons, corroborated by existing literatures such as *Adv. Funct. Mater.* **24**, 4681-4688 (2014) and *ACS Appl. Mater. Interfaces* **7**, 16750-16759 (2015). Moreover, transient electroluminescence decay curves (Supplementary Fig. 5) and the current-voltage characteristics of single-carrier devices (Supplementary Fig. 9) confirm our understanding that excitons recombine predominantly on the host material DMIC-TRZ, therefore electrons should be directly injected from POT2T into DMIC-TRZ just as you say.

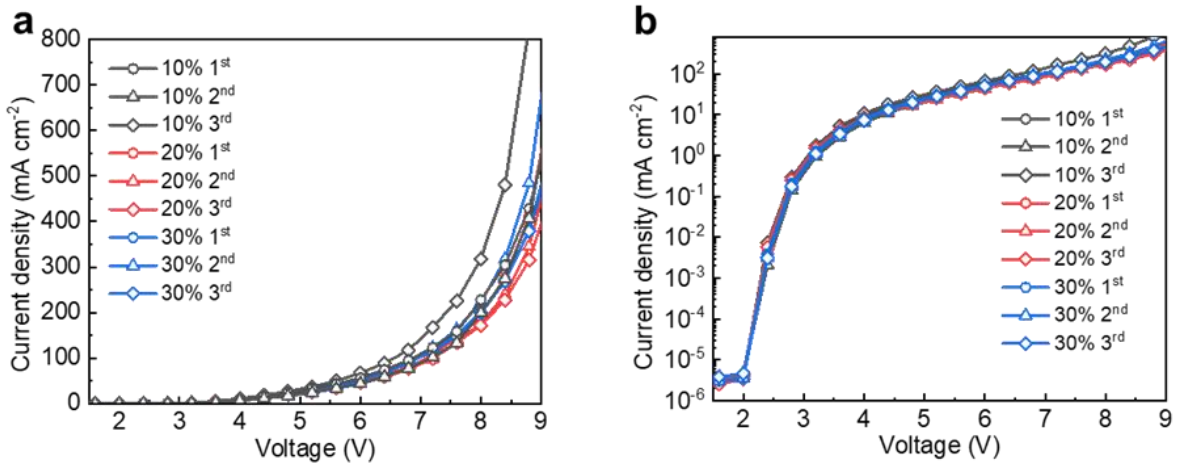

Fig. R5. Blue OLEDs without MR-Y. (a) Current density-voltage curves on a linear scale, (b) Current-density voltage curves on an exponential scale; The 1st, 2nd and 3rd represent three independent devices with the same structure.

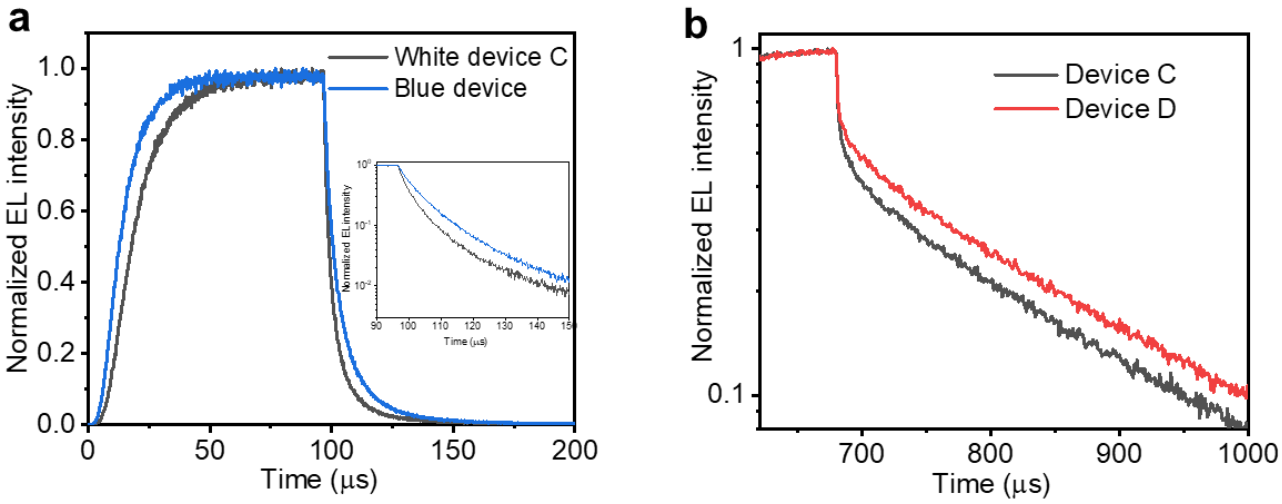

Supplementary Fig. 5. Transient EL decay curves. (a) Recorded at 490 nm with a pulse width of 200 μs for

white device C and blue device based on 20 wt% 5TCzBN:DMIC-TRZ as EML (b) Recorded at 550 nm with a pulse width of 1000 μs for white device C and D. Inset: Amplified EL decay curves following the withdrawn of pulse voltages.

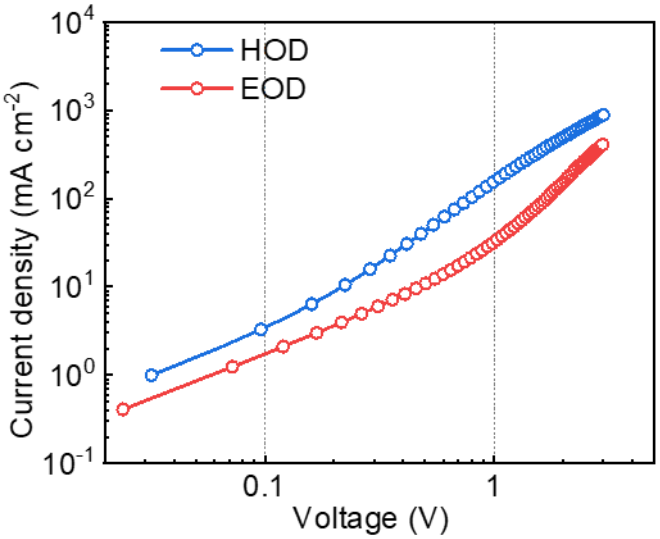

Supplementary Fig. 9. Current density-voltage characteristics of the hole-only device (HOD) and electron-only device (EOD). The device structure of the HOD and EOD were constructed as ITO/HATCN (5 nm)/TAPC (30 nm)/TCTA (15 nm)/mCBP (10 nm)/0.5 wt% MR-Y:20 wt% 5TCzBN:DMIC-TRZ (30 nm)/Al (100 nm) and ITO/0.5 wt% MR-Y:20 wt% 5TCzBN:DMIC-TRZ (30 nm)/POT2T (20 nm)/ANT-BIZ (30 nm)/Liq (2 nm)/Al (100 nm), respectively.

Comment 7: *It is suggested to add measurements of transient EL delay curves of devices with different EMLs to provide sufficient evidence for energy transfer from 5TCzBN to MR-Y.*

Response: According to your advice, we have included transient EL decay curves of related devices shown in Supplementary Fig. 5. In comparison to the blue device with only a blue light-emitting layer, device C exhibits fast transient EL decay at 490 nm, indicating efficient energy transfer from 5TCzBN to MR-Y. Furthermore, slower transient EL decay is observed at 550 nm in device D compared to device C, suggesting less effective triplet-to-singlet exciton conversion and increased accumulation of triplet excitons on MR-Y in device D, which was fabricated without 5TCzBN in the Y-EML. These results align with the observed trends of efficiency roll-offs in devices C and D, underscoring the pivotal role of 5TCzBN in the Y-EML and the occurrence of energy transfer from 5TCzBN to MR-Y.

Additional sentences (Manuscript, page 10): "Furthermore, device C exhibits fast transient EL decay at 490 nm, indicating efficient energy transfer from 5TCzBN to MR-Y (Supplementary Fig. 5). Device D, however, shows slower transient EL decay at 550 nm, suggesting less effective triplet-to-singlet exciton conversion and increased triplet exciton accumulation on MR-Y."

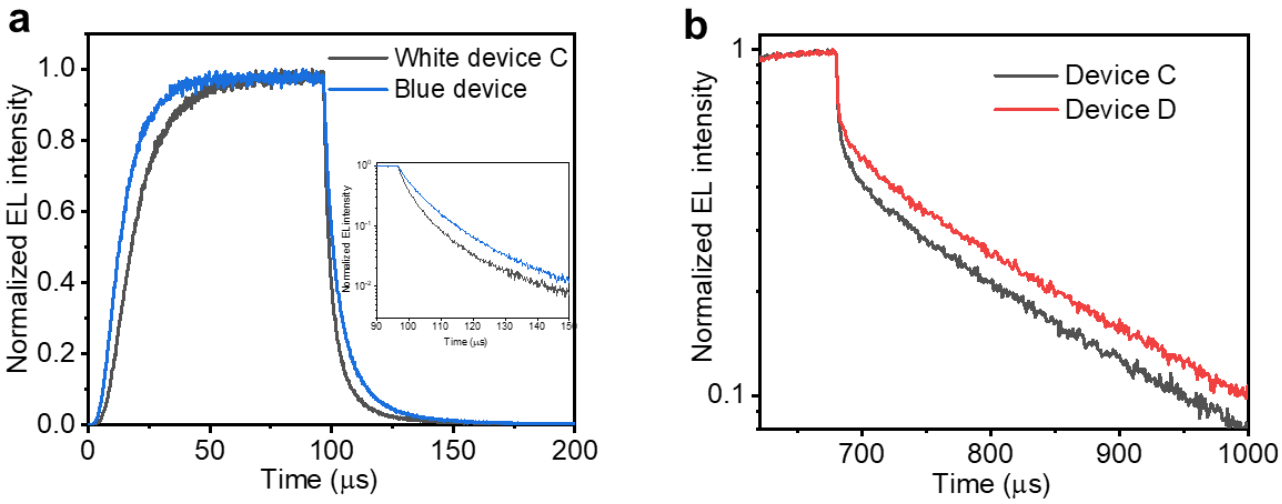

Supplementary Fig. 5. Transient EL decay curves. (a) Recorded at 490 nm with a pulse width of 200 μs for white device C and blue device based on 20 wt% 5TCzBN:DMIC-TRZ as EML (b) Recorded at 550 nm with a pulse width of 1000 μs for white device C and D. Inset: Amplified EL decay curves following the withdrawn of pulse voltages.

Comment 8: *Some numerical calculation formulas and calculation processes are not clear enough, such as k_r, k_{RISC} and Forster radius R_0. Please elaborate on the calculation process in the supplementary information.*

Response: We appreciate the reviewer for the constructive suggestion. Some detailed calculation formulas and step-by-step processes have been included in the supplementary information to elucidate these parameters comprehensively.

Additional section (supplementary information, supplementary note):

Supplementary Note 1. Analyses of Förster radius.

The rate of Förster-type energy transfer (k_{FET}) can be expressed as:

$$k_{FET} = k_{r,D}\frac{\kappa^2}{R^6}\left(\frac{9000(\ln 10)}{128\pi^5 N_A n^4}\right)\int_0^\infty F_D(\lambda)\varepsilon_A(\lambda)\lambda^4 d\lambda. \quad (S1)$$

where R is the intermolecular distance of the donor (5TCzBN or DMIC-TRZ) and acceptor (MR-Y); $k_{r,\mathrm{D}}$ is the radiative decay rate constant of the donor (5TCzBN or DMIC-TRZ) in absence of the acceptor (MR-Y); κ^2 is a configurational factor describing the relative orientation of electric transition dipole moments of the donor (5TCzBN or DMIC-TRZ) and acceptor (MR-Y) and is assumed to be 2/3 for a random distribution of the donor-acceptor pairs in our study; N_A is the Avogadro constant; n is the refractive index of the medium, for most of the organic materials is about 1.7; $F_\mathrm{D}(\lambda)$ is the normalized emission spectra of the donor (5TCzBN or DMIC-TRZ); $\varepsilon_\mathrm{A}(\lambda)$ is the molar absorption coefficient of the acceptor (MR-Y); and λ is the corresponding wavelength.

The Förster radius (R_0) is defined as an intermolecular distance at which the k_FET is equal to the $k_{r,\mathrm{D}}$.

Supplementary Note 2. Analyses of rate constants.

The respective rate constants of the prompt and delayed fluorescence components (k_p and k_d) occurring in the terminal emitter, can be given by:

$$k_\mathrm{p}, k_\mathrm{d} = \frac{k_{r,S} + k_{nr,S} + k_{ISC} + k_{r,T} + k_{nr,T} + k_{RISC}}{2} \times \left(1 \pm \sqrt{1 - \frac{4\left(k_{r,S} + k_{nr,S} + k_{ISC}\right)\left(k_{r,T} + k_{nr,T} + k_{RISC}\right) - 4k_{ISC}k_{RISC}}{\left(k_{r,S} + k_{nr,S} + k_{ISC} + k_{r,T} + k_{nr,T} + k_{RISC}\right)^2}} \right). \quad (S2)$$

k_p and k_d can be experimentally determined from prompt and delayed fluorescence decay time constants τ_p, τ_d as follows:

$$k_\mathrm{p} = \frac{1}{\tau_\mathrm{p}}. \quad (S3)$$

$$k_\mathrm{d} = \frac{1}{\tau_\mathrm{d}}. \quad (S4)$$

Besides, the emission quantum yields Φ_p and Φ_d for the prompt and delayed fluorescence components have the following relationship with these rate constants:

$$\Phi_\mathrm{p} = \frac{k_{r,S}}{k_\mathrm{p}} \frac{k_{r,S} + k_{nr,S} + k_{ISC} - k_d}{k_\mathrm{p} - k_\mathrm{d}}. \quad (S5)$$

$$\Phi_\mathrm{d} = \frac{k_{r,S}}{k_\mathrm{d}} \frac{k_p - k_{r,S} - k_{nr,S} - k_{ISC}}{k_\mathrm{p} - k_\mathrm{d}}. \quad (S6)$$

From the equations above, one could obtain the following relationship between rate constants and k_p, k_d, Φ_p and Φ_d experimentally determined from typical PLQY and transient PL characteristics:

$$k_{r,S} = \Phi_p k_p + \Phi_d k_d. \quad (S7)$$

$$k^S = k_{r,S} + k_{nr,S} + k_{ISC} = \frac{\Phi_p k_p^2 + \Phi_d k_d^2}{k_{r,S}}. \quad (S8)$$

$$k^T = k_{r,T} + k_{nr,T} + k_{RISC} = \frac{(\Phi_p + \Phi_d) k_p k_d}{k_{r,S}}. \quad (S9)$$

$$k_{ISC} k_{RISC} = \frac{\Phi_p \Phi_d k_p k_d (k_p - k_d)^2}{k_{r,S}^2}. \quad (S10)$$

In the presence of the yellow-light-emitting component (MR-TADF emitter), the respective rate constants of the prompt and delayed fluorescence components (k_p and k_d) occurring in the blue-light-emitting component (D-A type TADF emitter), can be given by:

$$k_p, k_d = \frac{k_{FET} + k_{r,S} + k_{nr,S} + k_{ISC} + k_{DET} + k_{r,T} + k_{nr,T} + k_{RISC}}{2} \times \left(1 \pm \sqrt{1 - \frac{4(k_{FET} + k_{r,S} + k_{nr,S} + k_{ISC})(K_{DET} + k_{r,T} + k_{nr,T} + k_{RISC}) - 4k_{ISC}k_{RISC}}{(k_{FET} + k_{r,S} + k_{nr,S} + k_{ISC} + k_{DET} + k_{r,T} + k_{nr,T} + k_{RISC})^2}}\right). \quad (S11)$$

Using Vieta's formula, the sum of k_p and k_d as well as the product of k_p and k_d can be expressed as:

$$k_p + k_d = k_{FET} + k_{r,S} + k_{nr,S} + k_{ISC} + k_{DET} + k_{r,T} + k_{nr,T} + k_{RISC}. \quad (S12)$$

$$k_p k_d = (k_{FET} + k_{r,S} + k_{nr,S} + k_{ISC})(k_{DET} + k_{r,T} + k_{nr,T} + k_{RISC}) - k_{ISC}k_{RISC}. \quad (S13)$$

By employing approximations, k_{FET} and k_{DET} can be simplified as follows:

$$k_{FET} = \frac{1}{\tau_{p,1}} - \frac{1}{\tau_{p,0}}. \quad (S14)$$

$$k_{DET} = \frac{1}{\tau_{d,1}} - \frac{1}{\tau_{d,0}} + k_{ISC}k_{RISC}(\tau_{p,1} - \tau_{p,0}). \quad (S15)$$

$\tau_{p,1}$ and $\tau_{p,0}$ represent prompt fluorescence decay times with or without guests, respectively. Likewise, $\tau_{d,1}$ and $\tau_{d,0}$ represent delayed fluorescence decay times with or without guests, respectively."

Comment 9: *Please supplement the current density-voltage-luminance (J-V-L) curves of all WOLEDs to better exhibit performance.*

Response: We appreciate the reviewer for the suggestion. Accordingly, we have included the current density-voltage-luminance (*J-V-L*) curves of all WOLEDs. These details are now comprehensively presented in the

Supplementary Information, specifically within Supplementary Figs. 1a, 2, 10c, 11b and 12a.

Comment 10: *To investigate the spatial distribution of exciton recombination in WOLEDs, ultrathin TBRb was employed. Please provide the detail information on the ultrathin TBRB and why it is located?*

Response: We thank the reviewer for the professional suggestion. Following this advice, we have provided the molecular structure of TBRb and its absorption spectrum in a dilute toluene solution, presented in Supplementary Fig. 7. The absorption spectrum of TBRb shows significant overlap with the emission spectrum of 5TCzBN, ensuring efficient energy transfer from 5TCzBN to TBRb. This suggests that TBRb has the potential to act as a detection for pinpointing the precise location of exciton recombination zones, as supported by existing literature (*Nat. Commun.* **13**, 5154 (2022)). Consequently, by analyzing the variation in EL intensity from TBRb at different spatial locations, we can deduce the spatial distribution of exciton recombination in WOLEDs.

Additional sentence, (manuscript, page 14): "Due to the fine overlap between the absorption spectrum of TBRb and the PL spectrum of 5TCzBN (Supplementary Fig. 7), efficient FET from 5TCzBN to TBRb could occur. The spatial distribution of excitons is characterized by the relative EL intensity of TBRb and 5TCzBN at different locations[8]."

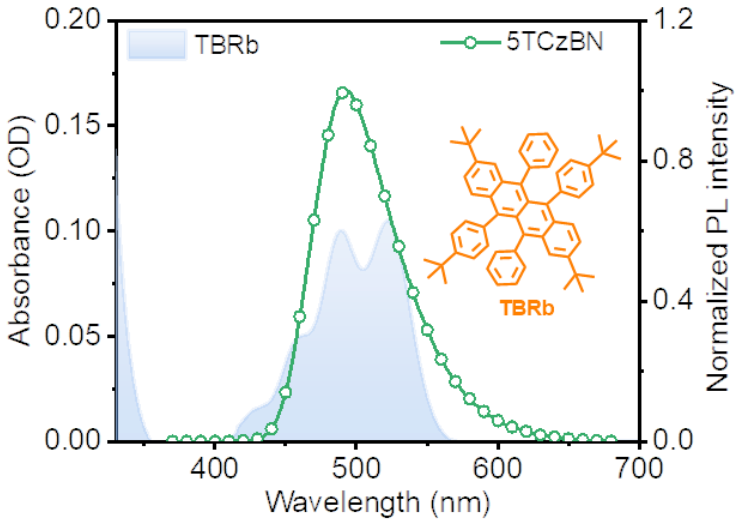

Supplementary Fig. 7. Absorption spectra of TBRb in the toluene dilute solution and emission spectra of 5TCzBN film.

REVIEWER COMMENTS

Reviewer #1 (Remarks to the Author):

Authors have well addressed the comments with sufficient supplementary experimental results, and the quality of the revised manuscript has been improved greatly. I recommend the acceptance of the manuscript at this stage.

Reviewer #2 (Remarks to the Author):

The author carefully responded to the reviewer's questions and added a lot of data. The reviewers believe that this manuscript can be published after correcting the following issues:

1) Table 1 should include device lifetime.

2） Table 2 should also include the photophysical properties of all ternary films, not just the binary films.

3) Why does the delayed fluorescence lifetime of MR-O doped films become longer after the introduction of sensitizers (Supplementary Fig. 14.)?

4) The authors mentioned that the three-color device mainly exhibits red emission （Fig. R2）, which is caused by exciton trapping within the red EML. So if the author swaps the positions of the red EML and the blue EML, can it be expressed as white emission?The authors should discuss the effect of the position of the different color EML in the three-color device.

Reviewer #3 (Remarks to the Author):

1. In Response 1, the authors mentioned “When considered alongside their close-to-ideal CIE coordinates (x and y values close to 0.33) at this brightness, our WOLEDs not only match but in some cases exceed the performance reported in the referenced studies.” and summarized the comparison of EQE, PE, and CIE with representative reports. From my perspective, comparing CIEx

and CIEy in different graphs is still meaningless. Please compare EQE (or PE), CIEx and CIEy in the same graph.

2. In Response 4, the authors interpreted “both the exciton recombination zone broadens and the exciton density rises, leading to an enhanced intensity of the blue light component. This increase in intensity is similarly observed in the yellow light component, as now detailed in Supplementary Fig. 8 of the revised supplementary information.” These explanations are reasonable. However, due to the spectral shape changing with the increase of the voltage, the authors should offer all the normalized EL spectra of WOLEDs in different voltages, not just one specific device.

3. On page 17, line 266, “In devices 265 G-1 and G-2, the EML consists of 0.3 wt% and 0.5 wt% MR-O doped into 20 wt% 50: DBFPO”. Is 50 correspond to mMDBA-DI? Please correct it.

Dear Editor and Reviewers,

Enclosed please find our revised manuscript entitled "**Harmonization of rapid triplet up-conversion and singlet radiation enables efficient and stable white OLEDs**" (Manuscript ID: **NCOMMS-23-50388B**) for consideration as a research article in ***Nature Communications***. We sincerely thank the reviewers for their further comments, which help us to improve the quality of our manuscript.

In response to the feedback from Reviewers #2 and #3, we have meticulously revised the manuscript and the point-by-point responses are provided. The major improvements include:

1. We have updated the tables to include device lifetimes and photophysical properties for all ternary films.
2. We have combined the EQEs (or PEs), CIE_x, and CIE_y into a single graph, with comparisons to existing references.
3. We have added the normalized EL spectra of all WOLEDs at different voltages.
4. We have fabricated and tested a three-color device with swapped positions of the red and blue emissive layer, as discussed in the response.

For your convenience, we have attached an annotated file of the revised manuscript and supporting information with all changes clearly highlighted. We hope that these revisions could satisfy the requirements for publication in ***Nature Communications***.

Yours Sincerely,

Chuluo Yang on behalf of the authors.

Corresponding author: **Professor Chuluo Yang**
at College of Materials Sciences and Engineering, Shenzhen University, Shenzhen 518071, People's Republic of China. Tel: +86-0755-86713985, e-mail: clyang@szu.edu.cn.

Reviewer #1:

General comment: *Authors have well addressed the comments with sufficient supplementary experimental results, and the quality of the revised manuscript has been improved greatly. I recommend the acceptance of the manuscript at this stage.*

Response: We sincerely appreciate the reviewer's positive and professional comment.

Reviewer #2:

General comment: *The author carefully responded to the reviewer's questions and added a lot of data. The reviewers believe that this manuscript can be published after correcting the following issues.*

Response: We sincerely appreciate the reviewer for the recognition of our work and the valuable comment.

Comment 1: *Table 1 should include device lifetime.*

Response: As suggested by the reviewer, we have updated **Table 1** to include the tested device lifetime data.

Modified table, (manuscript, Table 1):

Table 1 | Summary of the key performance data of WOLEDs.

Device	V_{on} (V)[a]	EQE (%)[b]	PE ($lm \cdot W^{-1}$)[c]	L_{max} ($cd \cdot m^{-2}$)[d]	CIE[e]	CCT (K)[e]	CRI[e]	LT_{80} (h)[f]
A	2.2	32.7/24.0	158/74	84009	(0.27, 0.46)	7217	41	-
B	2.2	35.9/27.6	184/95	127385	(0.31, 0.51)	5954	40	-
C	2.2	39.0/24.1	190/82	98134	(0.30, 0.49)	6343	41	446
D	2.2	38.5/16.3	196/52	103379	(0.33, 0.51)	5569	42	99
C-1	2.2	37.4/19.6	183/65	76662	(0.28, 0.47)	6833	42	-
C-2	2.2	38.5/22.7	194/79	105801	(0.30, 0.49)	6310	42	-
C-3	2.2	38.8/27.6	195/100	146016	(0.33, 0.52)	5616	40	-
C-4	2.2	37.1/30.7	194/112	132386	(0.35, 0.53)	5218	38	-
E	2.6	32.3/22.9	101/58	104673	(0.26, 0.46)	7444	42	-
F-1	2.4	34.5/18.9	117/44	111200	(0.38, 0.45)	4353	54	-
F-2	2.4	35.0/20.4	117/48	109769	(0.44, 0.46)	3362	47	-
F-3	2.2	33.6/16.7	130/41	67392	(0.30, 0.42)	6385	56	-
F-4	2.2	37.2/18.8	144/49	87713	(0.37, 0.45)	4632	56	-
G-1	3.0	35.8/26.0	78/35	64647	(0.26, 0.32)	120000	71	-
G-2	3.0	35.6/25.9	90/41	64647	(0.33, 0.34)	5583	69	-

[a] Turn-on voltage at 1 cd·m^{-2}; [b] External quantum efficiency: maximum, values at 1,000 cd·m^{-2}; [c] Power efficiency: maximum, values at 1,000 cd·m^{-2}; [d] Maximum luminance; [e] Commission Internationale de l'Eclairage coordinates, correlated color temperature and color rendering index at 1,000 cd·m^{-2}. [f] Operational time to 80% of the initial luminance of 1,000 cd·m^{-2}.

Comment 2: *Table 2 should also include the photophysical properties of all ternary films, not just the binary films.*

Response: According to your suggestion, we have updated **Table 2** to include the tested photophysical properties of all ternary films. The corresponding columns for Φ_p, Φ_d, and rate constants are left blank. This is because the complexity of the energy transfer process in ternary films makes it meaningless to calculate them based on the PLQY and transient PL data.

Modified table, (manuscript, Table 2):

Table 2 | Transient PL characteristic and rate constants of films.

Film	λ_{max}[a] (nm)	τ_p[b] (ns)	τ_d[b] (μs)	Φ_{PL}[c] (%)	Φ_p[d] (%)	Φ_d[d] (%)	$k_{r,S}$[e] × 10^7 (s^{-1})	k_{ISC}[e] × 10^7 (s^{-1})	k_{RISC}[e] × 10^4 (s^{-1})	k_{FET}[f] × 10^6 (s^{-1})	k_{DET}[f] × 10^5 (s^{-1})
20 wt% 5TCzBN:DMIC-TRZ	490	17.0	5.8	63	18	45	1.0	4.2	61	56.1	2.4
0.5 wt% MR-Y:20 wt% 5TCzBN:DMIC-TRZ	490/ 550	8.7/ 3.5	1.6/ 3.4, 110.0	95	-	-	-	-	-		
0.5 wt% MR-Y:DMIC-TRZ	550	8.1	140.0	98	44	54	5.4	6.8	1.6	-	-
20 wt% *m*MDBA-DI:DBFPO	466	47.3	2.5	97	25	72	0.6	1.4	149	7.5	2.4
0.5 wt% MR-O:20 wt% *m*MDBA-DI:DBFPO	466/ 580	34.9/ 4.6	1.1/ 2.4, 109.0	93	-	-	-	-	-		
0.5 wt% MR-O:DBFPO	580	7.1	117.0	97	51	46	7.2	6.6	1.6	-	-

[a] Peak wavelength of the PL spectrum in the film; [b] Lifetime of the prompt component and delayed component determined from the transient PL decay curve at 298 K; [c] Absolute photoluminescence quantum yield measured with an integration-sphere system under argon atmosphere; [d] Absolute photoluminescence quantum yield of prompt fluorescence and delayed fluorescence; [e] Rate constants of singlet radiative decay, intersystem crossing and reverse intersystem crossing. [f] Rate constants of Förster energy transfer and Dexter energy transfer.

Comment 3: *Why does the delayed fluorescence lifetime of MR-O doped films become longer after the introduction of sensitizers (Supplementary Fig. 14.)?*

Response: We appreciate the reviewer for the insightful question. It appears that the transient PL decay curves

at the emission wavelength of 580 nm in the previous submission were abnormal, likely due to residual oxygen during testing or an artifact of our film fabrication or measurement setup. In response, we have prepared new films and ensured complete deoxygenation during retesting (**Supplementary Fig. 14b and Table 2**). We find that the PL decay curve for the ternary film fits a tri-exponential model better, yielding delayed fluorescence lifetimes of 2.4 μs and 109.0 μs. These lifetimes suggest involvement of multiple luminescent processes. The shorter lifetime (2.4 μs) likely corresponds to the excitons experiencing FET from the sensitizer *m*MDBA-DI to MR-O, immediately followed by radiative decay from the S_1 to S_0 state of MR-O (Fig. R1a). This rapid transition aligns with the fluorescence lifetime of the sensitizer alone. The longer lifetime (109.0 μs) corresponds to excitons that initially transfer to the S_1 state of MR-O and then undergo the ISC process to reach the T_1 state of MR-O. Subsequently, these excitons in the T_1 state of MR-O are upconverted back to the S_1 state of MR-O, emitting delayed fluorescence (Fig. R1b). This results in a prolonged fluorescence lifetime, comparable to that observed in binary films.

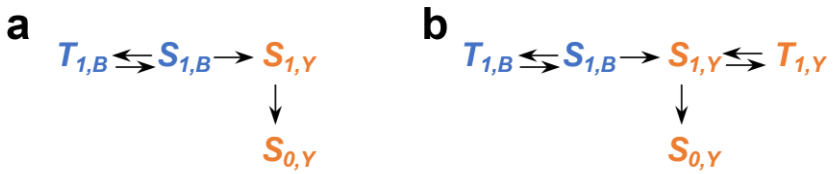

Fig. R1. The schematic diagram of luminescent processes in the ternary film. $S_{1,B}$ and $T_{1,B}$ represent the singlet state and triplet state of *m*MDBA-DI, respectively. $S_{1,Y}$, $T_{1,Y}$, and $S_{0,Y}$ represent the singlet state, triplet state and ground state of MR-O, respectively.

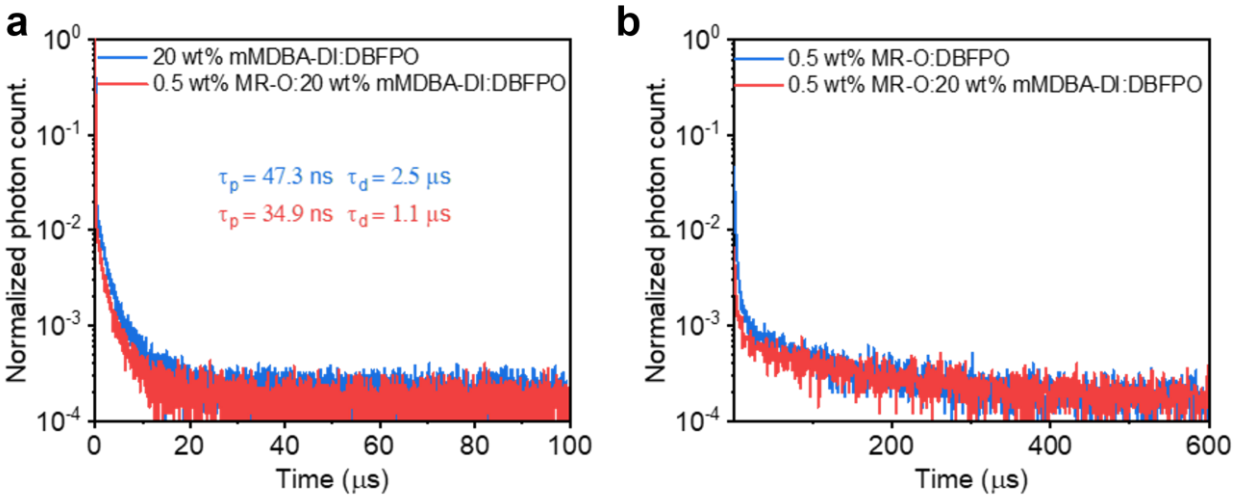

Supplementary Fig. 14. Transient PL decay curves. (a) The films with or without MR-O doping in the 20 wt% *m*MDBA-DI:DBFPO matrix at the emission wavelength of 466 nm. (b) The films with MR-O doping in

the DBFPO and 20 wt% *m*MDBA-DI:DBFPO matrix at the emission wavelength of 580 nm.

Comment 4: *The authors mentioned that the three-color device mainly exhibits red emission （Fig. R2）, which is caused by exciton trapping within the red EML. So if the author swaps the positions of the red EML and the blue EML, can it be expressed as white emission? The authors should discuss the effect of the position of the different color EML in the three-color device.*

Response: We appreciate the reviewer's emphasis on the significance of the EML positions in the three-color device. Following your suggestion, we swap the positions of the red EML and the blue EML to fabricate device denoted as **three color-2**. As expected, the device **three color-2** shows more intense blue and yellow emissions (Fig. R2) compared to device **three color-1**, resulting in a warm white emission with a CIE coordinate of (0.41, 0.45). This demonstrates that the arrangement of EMLs significantly impacts the device's emission characteristics, shedding light on pivotal considerations for our future device designs.

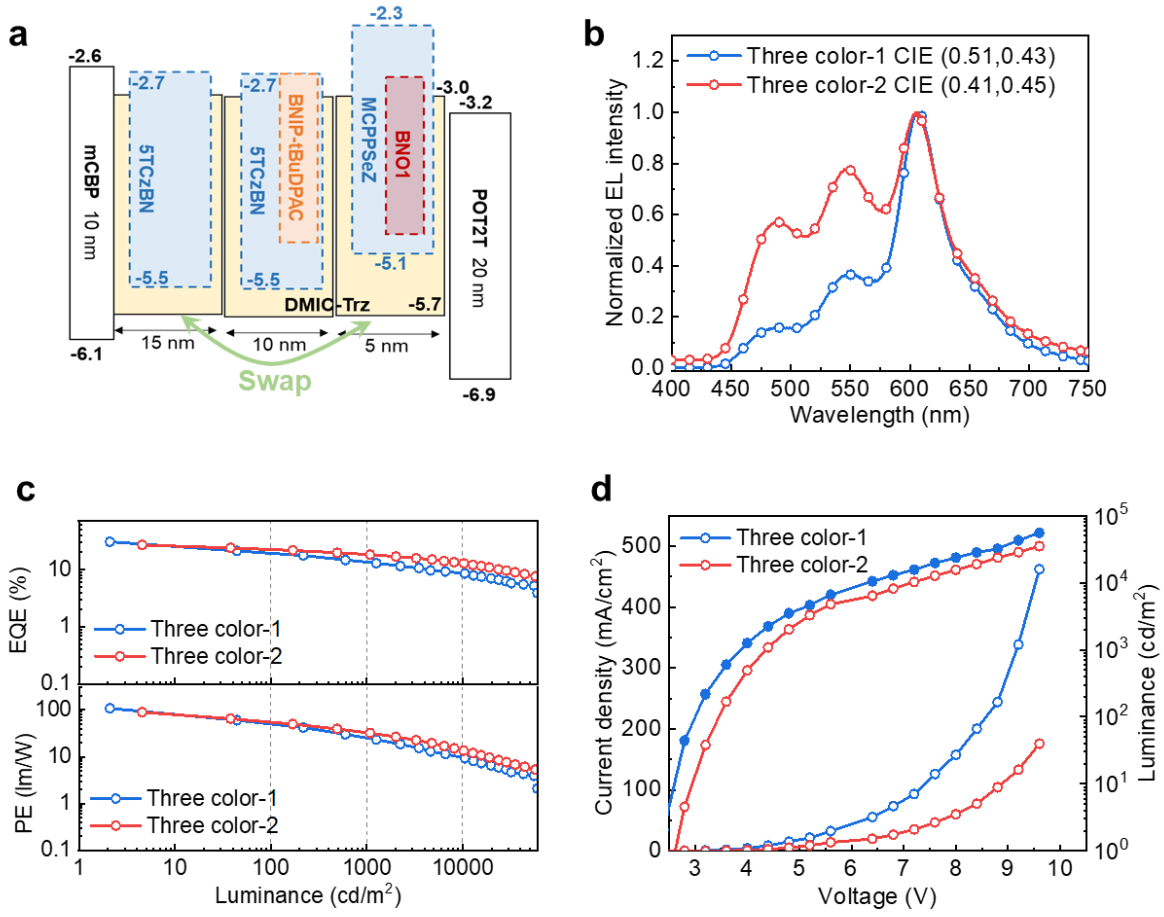

Fig. R2. Three-color WOLEDs. a, Device architectures. For device three color-1, the red EML consisted of 0.5 wt% BNO1:20 wt% MCPPSeZ:DMIC-TRZ is placed near the hole-blocking layer (HBL). Conversely, the

red EML of device three color-2 is located near the electron-blocking layer (EBL) **b**, Normalized electroluminescent spectra. **c**, EQE and PE versus luminance characteristics. **d**, Current density-voltage-luminance curves for three color-1 and three color-2.

Reviewer #3:

Comment 1: *In Response 1, the authors mentioned "When considered alongside their close-to-ideal CIE coordinates (x and y values close to 0.33) at this brightness, our WOLEDs not only match but in some cases exceed the performance reported in the referenced studies." and summarized the comparison of EQE, PE, and CIE with representative reports. From my perspective, comparing CIE_x and CIE_y in different graphs is still meaningless. Please compare EQE (or PE), CIE_x and CIE_y in the same graph.*

Response: We appreciate the reviewer for the constructive suggestions. In the updated version, we have provided three-dimensional graphs that map EQE (or PE) against CIE_x and CIE_y, as shown in **Supplementary Fig. 16**. These visualizations clearly demonstrate that our WOLEDs not only match the performance reported in referenced studies but also exhibit CIE_x and CIE_y values closer to the blackbody radiation curve, aligning nearer to the ideal white light coordinates of (0.33, 0.33).

Modified graph, (Supplementary Information, Supplementary Fig. 16):

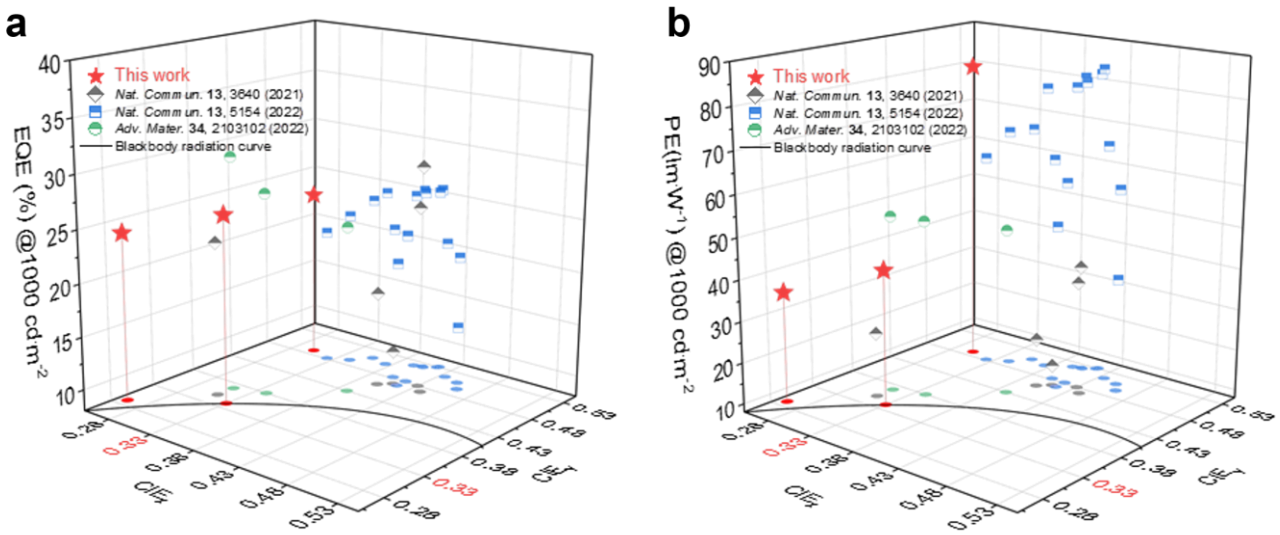

Supplementary Fig. 16. Comparison of EQE, PE, and CIE with representative reports. (a) EQE_{1000} versus CIE_x and CIE_y coordinates at the luminance of 1,000 $cd \cdot m^{-2}$. (b) PE_{1000} versus CIE_x and CIE_y coordinates at the luminance of 1,000 $cd \cdot m^{-2}$.

Comment 2: *In Response 4, the authors interpreted "both the exciton recombination zone broadens and the exciton density rises, leading to an enhanced intensity of the blue light component. This increase in intensity is similarly observed in the yellow light component, as now detailed in Supplementary Fig. 8 of the revised supplementary information." These explanations are reasonable. However, due to the spectral shape changing with the increase of the voltage, the authors should offer all the normalized EL spectra of WOLEDs in different voltages, not just one specific device.*

Response: We appreciate the reviewer for the professional suggestion. All normalized EL spectra of WOLEDs in different voltages have been supplemented in the revised supplementary information. Additionally, we have also updated the manuscript with descriptions relevant to the newly added graphs.

Modified sentences (Manuscript, page 6): "The current density-voltage-luminance (*J*-*V*-*L*) characteristics and normalized electroluminescence (EL) spectra of devices A and B at different voltages are illustrated in Supplementary Figs. 2a~2c."

Modified sentences (Manuscript, page 7): "with their performances depicted in Fig. 3 and Supplementary Figs. 2d~2f."

Modified graphs (Supplementary information, Supplementary Fig. 2, Supplementary Fig. 10, Supplementary Fig. 11)

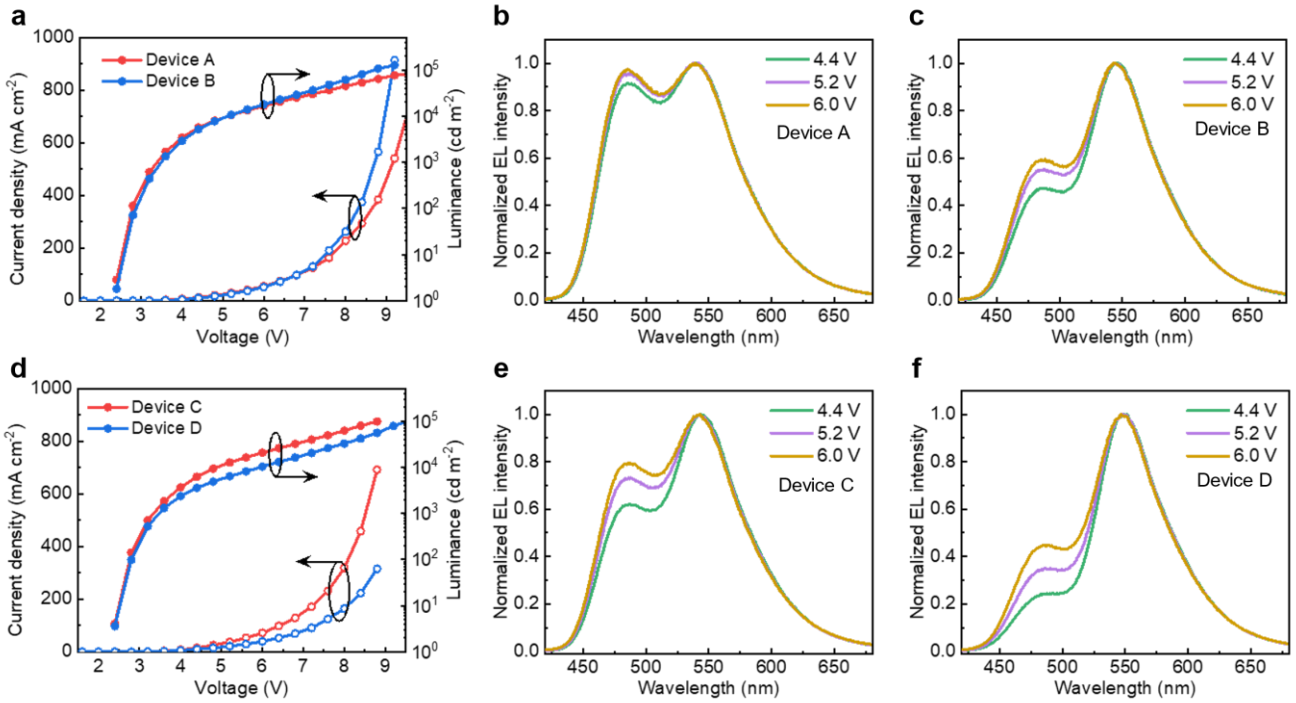

Supplementary Fig. 2. WOLEDs (devices A-D). (a) Current density-voltage-luminance (*J-V-L*) curves and normalized EL spectra at different voltages of (b) devices A and (c) devices B. (d) Current density-voltage-luminance (*J-V-L*) curves and normalized EL spectra at different voltages of (e) devices C and (f) devices D.

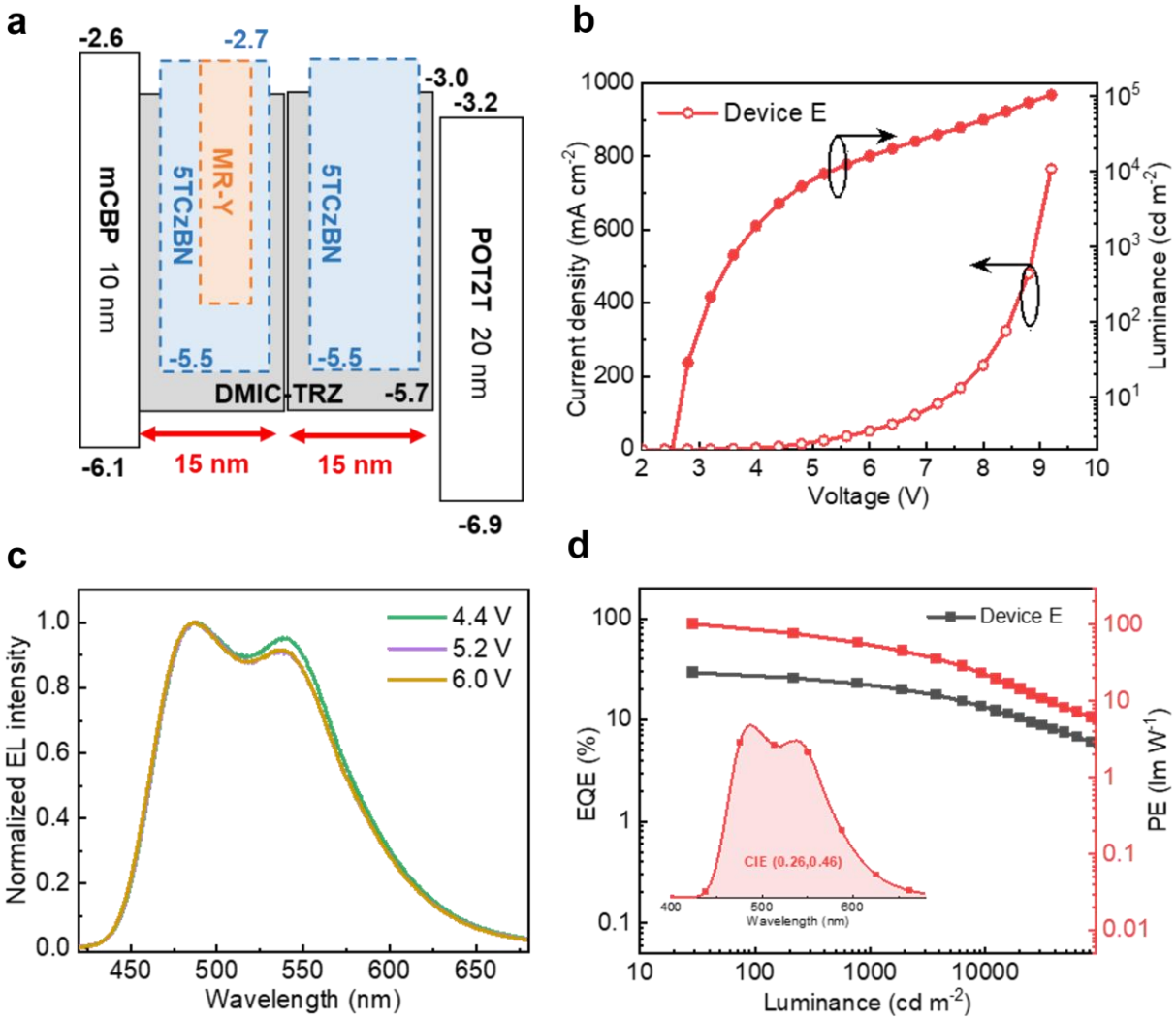

Supplementary Fig. 10. WOLED (device E). (a) The device configuration. (b) *J-V-L* curves. (c) Normalized EL spectra at different voltages. (d) EQE and PE versus luminance characteristics. The inset is normalized EL spectra tested at 1000 cd·m^{-2} for device E.

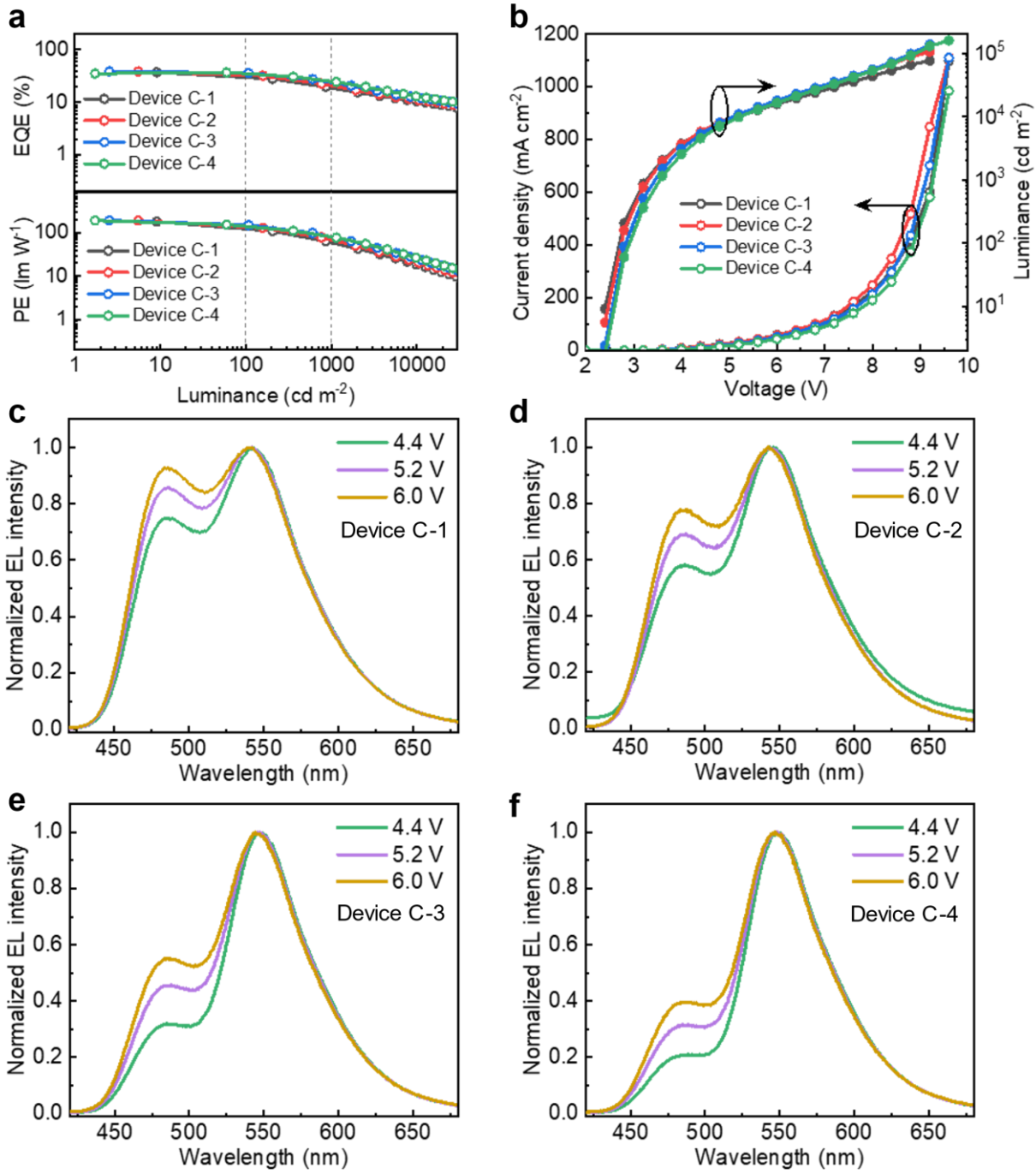

Supplementary Fig. 11. WOLED (device C-1~4). (a) EQE and PE versus luminance characteristics and (b) *J-V-L* curves of devices C-1~4. Normalized EL spectra at different voltages for (c) device C-1, (d) device C-2, (e) device C-3 and (f) device C-4.

Comment 3: *On page 17, line 266, "In devices 265 G-1 and G-2, the EML consists of 0.3 wt% and 0.5 wt% MR-O doped into 20 wt% 50: DBFPO". Is 50 correspond to mMDBA-DI? Please correct it.*

Response: Thank you for pointing out this error. The mistake has been corrected and highlighted in our revised manuscript.

Modified sentences (Manuscript, page 11): "In devices G-1 and G-2, the EML consists of 0.3 wt% and 0.5 wt% MR-O doped into 20 wt% *m*MDBA-DI:DBFPO"

We believe that these revisions fully address the reviewer's concerns and enhance the overall presentation of our work. We appreciate the reviewer's positive evaluation and valuable suggestions, which have greatly helped us refine our manuscript for publication.

REVIEWERS' COMMENTS

Reviewer #2 (Remarks to the Author):

The authors carefully revised the manuscript based on the reviewers' comments. The reviewer believes that this manuscript can be accepted at this stage.

Reviewer #3 (Remarks to the Author):

The authors have revised the manuscript properly. It can be accepted now.